Supporting Information

Co(II)-embedded covalent organic framework for catalyzing CO_2 fixation to highly valuable N-formamides and 2-oxazolidinones under mild conditions

Vaibhav Parihar, Shubham Kumar, Pooja Rani and C. M. Nagaraja*

Department of Chemistry, Indian Institute of Technology Ropar, Rupnagar 140001, Punjab, India. Tel: 91-1881-232057. Email: cmnraja@iitrpr.ac.in

Table of contents

Physical measurements

Powder X-ray diffraction (PXRD) measurements were conducted in the 2θ range of 2-30° on PANanalytical's X'PERT PRO X-Ray diffractometer with a scan rate of 2°/min using Cu-Kα radiation (λ = 1.54184 Å, 40 kV, 20 mA). PXRD patterns of COF after thermal treatment under vacuum at 50, 100, 150, and 200 °C using a degassing setup were recorded after cooling to room temperature. Fourier transform infrared (FT-IR) spectra of the samples were recorded on a Bruker Tensor-F27 instrument in ATR mode. The FE-SEM images and EDAX patterns were recorded on the JEOL JSM-7610F instrument. The TEM images were recorded on the Thermo Scientific Themis 300 Kv instrument. The metal content of Co(II) in the COF was determined by Agilent's microwave-plasma atomic emission spectrometer (MP-AES). X-ray photoelectron spectroscopy (XPS) analyses were performed on a Thermo Fisher Scientific NEXSA photoemission spectrometer using Al Kα (1486.6 eV) X-ray radiation.

Thermogravimetric analyses of the COF samples were carried out using a Metler Toledo thermogravimetric analyzer under an air atmosphere with a flow rate of 30 mL/min and a temperature range of 25-800 °C (heating rate of 5 °C/min). The ^{13}C CP-MAS (Cross Polarization Magic Angle Spinning) solid-state NMR spectra were recorded on a 600 MHz high-field NMR spectrometer (JNM-ECZ600R/M3) instrument.

Experimental section

Materials

All the chemicals used in this work were commercially available, of analytical grade, and were used as received without further purification. 4,4′,4″,4‴-(ethene-1,1,2,2-tetrayl)-tetraaniline (ET-NH_2) and 2,5-dihydroxyterephthalaldehyde (Dh-CHO) were purchased from Chem Scene. $Co(OAc)_2.4H_2O$ was purchased from Sigma Aldrich Chemicals Co. Acetic acid (99%), 1,4-dioxane, and $PhSiH_3$ were purchased from Merck and Co. All the amines used for the N-formylation reaction were purchased from TCI India.

Synthesis of EtDh-COF

The EtDh-COF was synthesized by following the reported procedure with a slight modification.[1] Typically, 4,4′,4″,4‴-(ethene-1,1,2,2-tetrayl)-tetraaniline (ET-NH_2) (30 mg, 0.0764 mmol) and 2,5-dihydroxyterephthalaldehyde (Dh-CHO) (25.4 mg, 0.153 mmol) were charged to a Pyrex tube to which 1 mL of 1,4-dioxane was added and sonicated for 15 min to get a homogenous mixture. Then, the tube was flash-frozen at 77 K using a liquid N_2 bath, degassed by freeze-pump-thaw for three cycles, and sealed. The tube was placed in a preheated oven at 120 °C without disturbance for 3 days to obtain a reddish-orange solid, which was isolated by filtration and washed with 1,4-dioxane to remove any unreacted reagents. The obtained solid powder was dried under vacuum at 100°C for 2 h to get EtDh-COF.

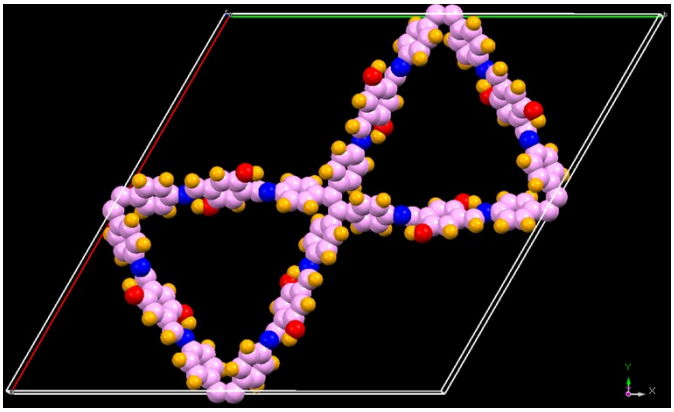

Figure S1. The unit cell of EtDh-COF (light pink, C; yellow, H; blue, N; red, O).

Table S1. Fractional atomic coordinates of EtDh-COF.

Crystal system: *Hexagonal*
Space groups: *P6*
Cell Parameters: $a = b = 38.9$ Å; $c = 5.2$ Å; $\alpha = \beta = 90°$, $\gamma = 120°$

Atoms	***x***	***y***	***z***
C	1.03428	0.47783	0.47965
C	1.06312	0.49601	0.67382
C	1.09754	0.49275	0.68026
C	1.10426	0.47115	0.48989
C	1.07540	0.45255	0.29457
C	1.04087	0.45575	0.29044
C	1.26315	0.48270	0.27998
C	1.22818	0.48357	0.22599
C	1.19413	0.46320	0.38199
C	1.19584	0.44100	0.59197
C	1.23066	0.43980	0.64445
C	1.26520	0.46061	0.49133
C	1.29914	0.45800	0.55740
C	1.16013	0.46571	0.32285
O	1.16423	0.41980	0.74679
O	1.29390	0.50411	0.11957
N	1.13784	0.46911	0.50952
N	1.33345	0.47641	0.42526
C	1.36852	0.47687	0.45519
C	1.37648	0.45576	0.64446
C	1.41368	0.45775	0.65366
C	1.44412	0.48077	0.47492
C	1.43564	0.50188	0.28901
C	1.39870	0.50018	0.27886
C	1.48122	0.48171	0.47771
H	1.05907	0.51182	0.81248
H	1.11794	0.50648	0.82358

H	1.07971	0.43625	0.15645
H	1.02084	0.44172	0.14770
H	1.22798	0.49970	0.07113
H	1.23039	0.42341	0.79884
H	1.29740	0.44120	0.71313
H	1.15337	0.46681	0.13416
H	1.14031	0.42121	0.71349
H	1.31872	0.50465	0.15198
H	1.35525	0.43868	0.77575
H	1.41828	0.44196	0.79232
H	1.45649	0.51871	0.15811
H	1.39384	0.51599	0.14065

Synthesis of Co-COF

In a 50 mL two-neck round-bottom flask, EtDh-COF (0.04 mmol) and $Co(OAc)_2.4H_2O$ (0.24 mmol) were mixed in 20 mL of ethanol under an inert atmosphere, and the resulting reaction mixture was refluxed for 12 h. After cooling to room temperature, the product was isolated by filtration and washed with excess ethanol to remove any unreacted reagents. The reddish-brown solid of Co-COF obtained was dried under a vacuum at 100°C for 12 h. The Co(II) content in the COF was estimated by MP-AES analysis.

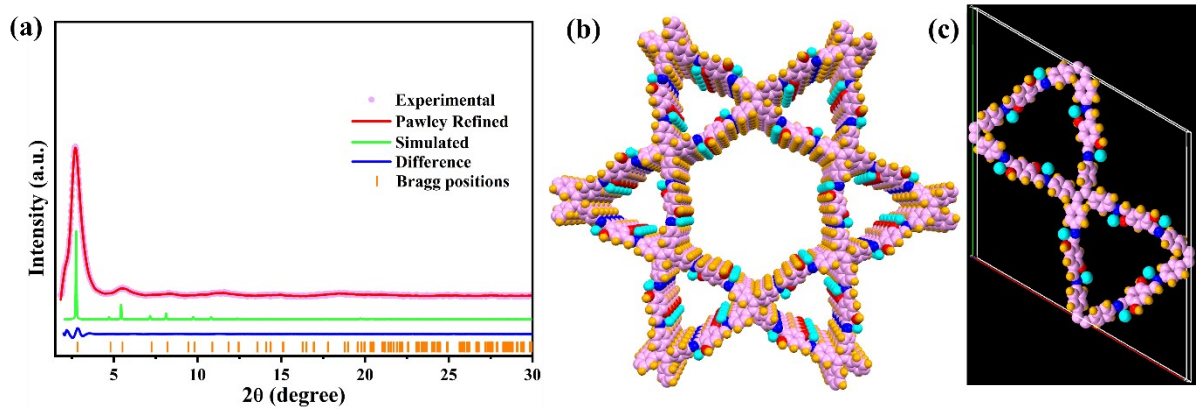

Figure S2. (a) Comparison of theoretical and experimental PXRD patterns, (b) Graphic extended view of AA-stacking mode, and (c) Unit cell of Co-COF (light pink, C; yellow, H; blue, N; red, O; cyan, Co).

Table S2. Fractional atomic coordinates of Co-COF.

Crystal system: *Hexagonal*
Space groups: *P6*
Cell Parameters: *a = b = 38.9 Å; c = 5.2 Å; α = β = 90°, γ = 120°*

Atoms	***x***	***y***	***z***
C	1.03429	0.47781	0.47963
C	1.06318	0.49601	0.67415
C	1.09758	0.49274	0.68027
C	1.10427	0.47116	0.48989
C	1.07541	0.45254	0.29456
C	1.04088	0.45574	0.29043
C	1.26314	0.48271	0.27997
C	1.22819	0.48358	0.22598
C	1.19414	0.46321	0.38198
C	1.19585	0.44101	0.59198
C	1.23067	0.43981	0.64446
C	1.26521	0.46062	0.49132
C	1.29914	0.45801	0.55739
C	1.16014	0.46572	0.32284
O	1.16424	0.41980	0.74679
O	1.29391	0.50411	0.11957
N	1.13785	0.46912	0.50952
N	1.33346	0.47642	0.42526
C	1.36853	0.47687	0.45518
C	1.37649	0.45577	0.64446
C	1.41368	0.45776	0.65366
C	1.44413	0.48078	0.47492
C	1.43565	0.50188	0.28901
C	1.39871	0.50018	0.27886
C	1.48123	0.48171	0.47771
H	1.05908	0.51182	0.81247
H	1.11795	0.50649	0.82358
H	1.07972	0.43625	0.15645
H	1.02085	0.44172	0.14770
H	1.22799	0.49970	0.07113
H	1.23040	0.42341	0.79884
H	1.29741	0.44120	0.71313
H	1.15338	0.46681	0.13416
H	1.16631	0.40799	0.90721
H	1.29001	0.50770	-0.06054
H	1.35526	0.43868	0.77575
H	1.41829	0.44196	0.79232
H	1.45650	0.51871	0.15811
H	1.39385	0.51599	0.14065
Co	1.11421	0.41438	0.62816
Co	1.34664	0.52734	0.27242

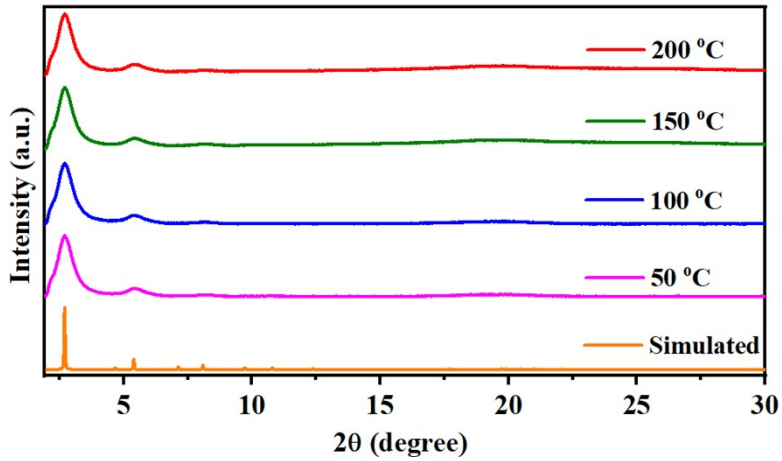

Figure S3. PXRD patterns of COF after thermal treatment under vacuum at 50, 100, 150, and 200 °C using a degassing setup.

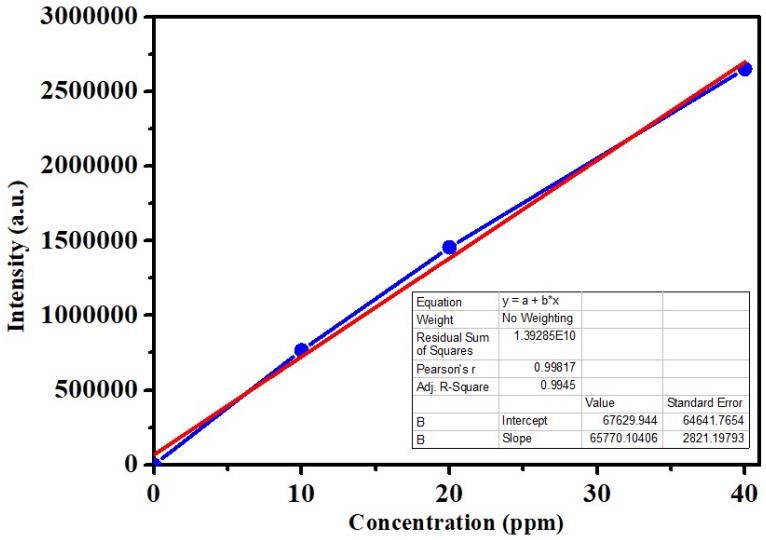

Figure S4. MP-AES calibration curve for Co-COF.

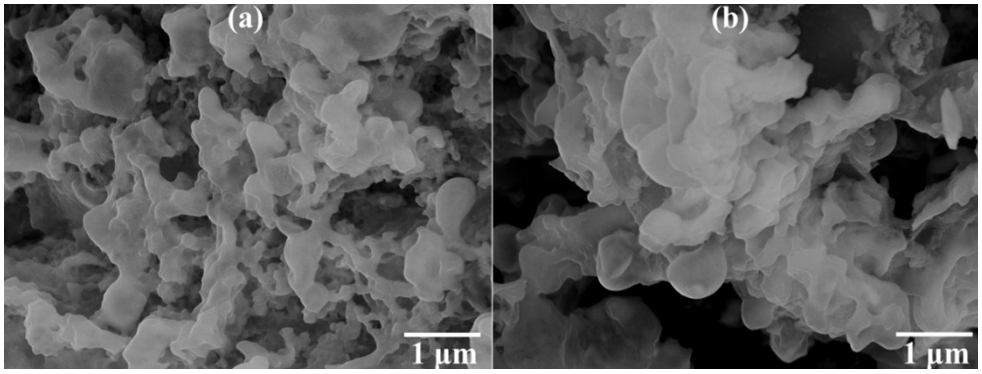

Figure S5. FE-SEM image of (a) EtDh-COF, and (b) Co-COF.

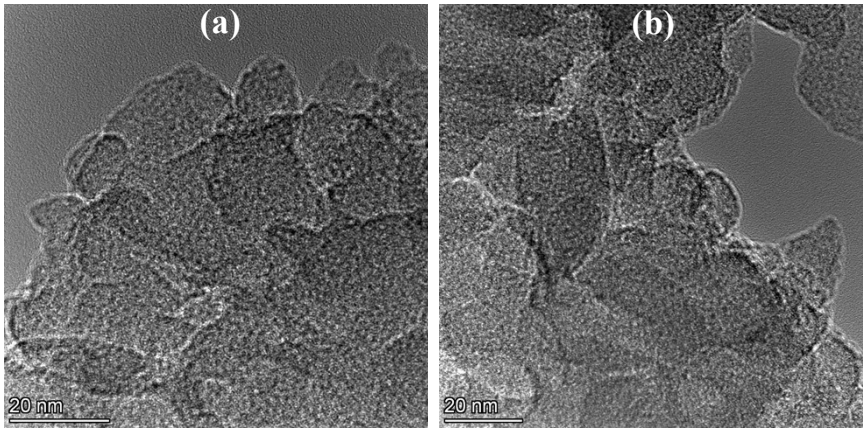

Figure S6. HR-TEM image of (a) EtDh-COF, and (b) Co-COF.

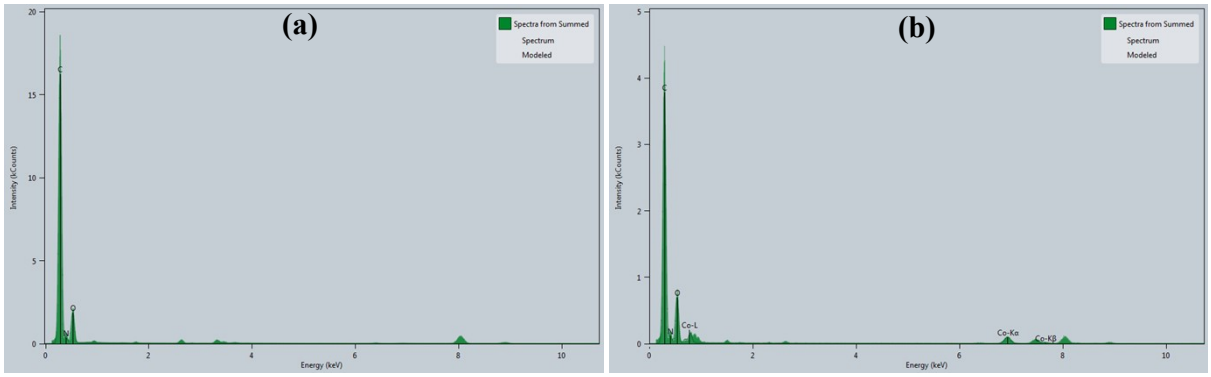

Figure S7. EDS plot of (a) EtDh-COF, and (b) Co-COF.

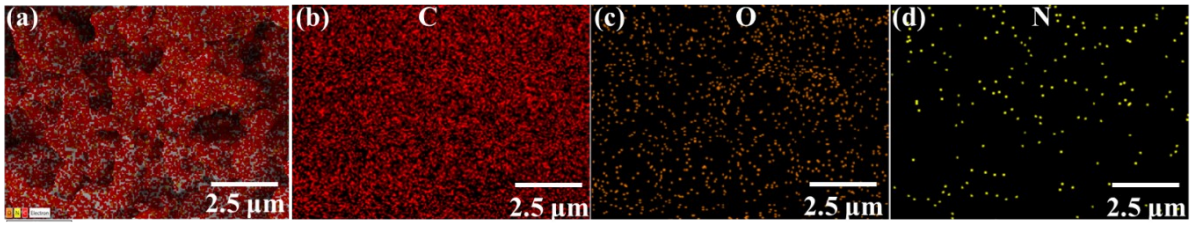

Figure S8. Elemental mapping of EtDh-COF (a) representing C (b), O (c), and N (d).

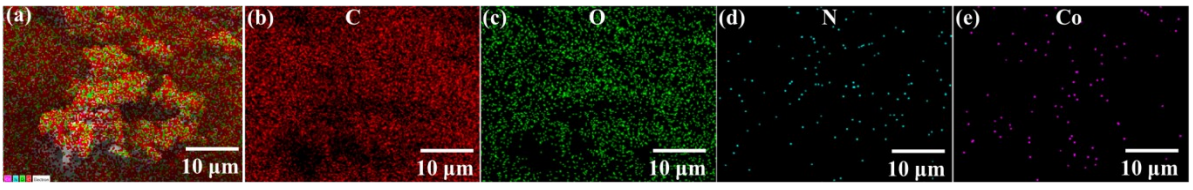

Figure S9. Elemental mapping of Co-COF (a) representing C (b), O (c), N (d), and Co (e).

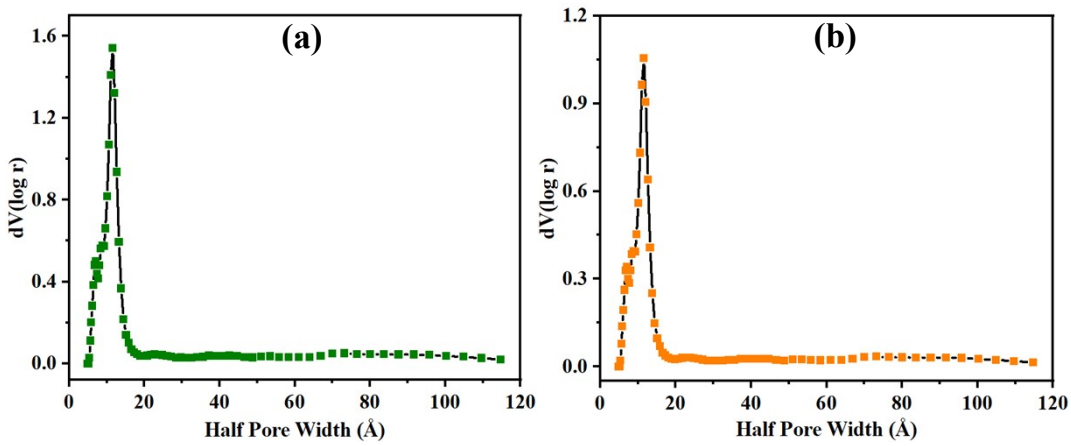

Figure S10. Pore size distribution plots of (a) EtDh-COF, and (b) Co-COF.

Adsorption measurements

N_2 adsorption-desorption measurements were performed at 77 K on a Quantachrome QUADRASORB-SI automatic volumetric instrument. Ultrapure (99.995%) N_2 and CO_2 gases were used for the isotherm measurements. Before starting the adsorption measurements, the COF samples were exchanged with dry methanol for 24 h and activated at 120 °C under a vacuum for 12 h. The activated sample was connected to the surface area analyzer, and all the operations were computer-controlled. The temperature of 77 K was achieved using liquid nitrogen. The 273 K and 298 K temperatures were reached using a chiller with a water and ethylene glycol mixture (1:1 v/v mixture).

Analysis of gas adsorption isotherms

The Clausius-Clapeyron equation[2] was used to calculate the enthalpies of carbon dioxide adsorption.[3] Using the Langmuir-Freundlich equation, an accurate fit was retrieved to predict CO_2 adsorbed at saturation precisely. A modification of the Clausius-Clapeyron equation was used for the calculations.

$$ln(P1/P2) = \Delta H_{ads}(T2 - T1/R.T1.T2) \quad \text{.....(i)}$$

where P_1 and P_2 = Pressures for isotherm at 273 K and 298 K, respectively.

T_1 and T_2 = Temperatures for isotherms at 273 K and 298 K, respectively.

ΔH_{ads} = Enthalpy of adsorption.

R = Universal gas constant = 8.314 J/K/mol).

The pressure is a function of the amount of gas adsorbed, which was determined by using a Langmuir-Freundlich fit.

$$Q/Q_m = B.P^{(1/t)}/1 + (B.P^{(1/t)}) \quad \ldots\ldots \text{(ii)}$$

where Q = moles of gas adsorbed

Q_m = moles of gas adsorbed at saturation

B and t = constants

P = Pressure

By rearranging equation (ii) we get equation (iii)

$$P = [(Q/Q_m)/\{B - (B.(Q/Q_m)\}]^t \quad \ldots\ldots\ldots\text{(iii)}$$

Substituting equation (iii) into equation (i) we get

$$\Delta H_{ads} = \{R.T1.T2/(T2 - T1)\}.ln\frac{[(Q/Q_{m1})/\{B - (B.Q/Q_{m1})\}]^{t1}}{[(Q/Q_{m2})/\{B - (B.Q/Q_{m2})\}]^{t2}} \quad \ldots\ldots\ldots\text{(iv)}$$

In equation (iv), subscripts 1 and 2 represent data corresponding to 273 K and 298 K, respectively.

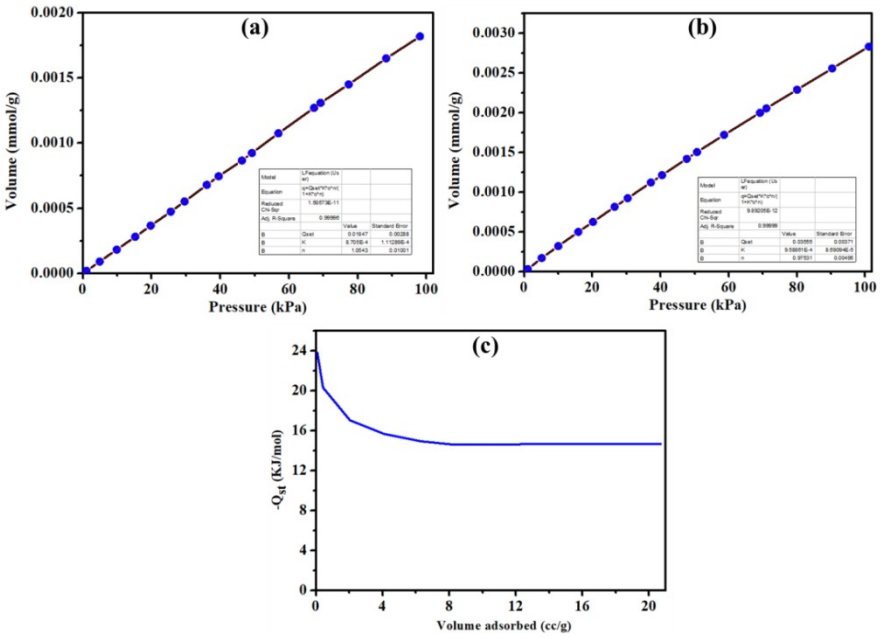

Figure S11. Carbon dioxide adsorption isotherm for EtDh-COF carried out at (a) 298 K and (ii) 273 K (the solid line shows the best fit to the data using the Langmuir-Freundlich equation), and (c) the enthalpy of carbon dioxide adsorption for EtDh-COF computed using the Clausius-Clapeyron equation.

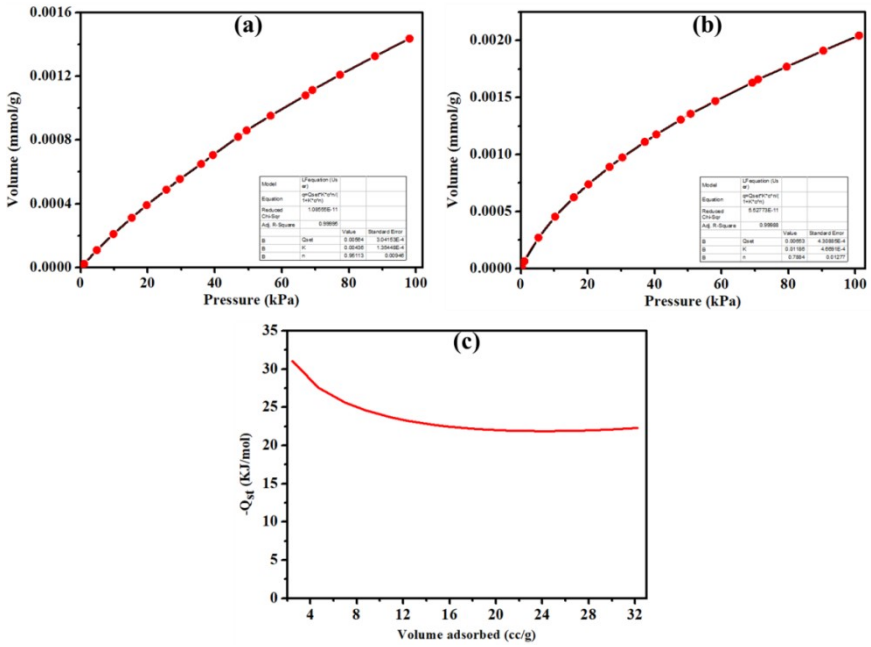

Figure S12. Carbon dioxide adsorption isotherm for Co-COF carried out at (a) 298 K and (b) 273 K (the solid line shows the best fit to the data using the Langmuir-Freundlich equation), and (c) the enthalpy of carbon dioxide adsorption for Co-COF computed using the Clausius-Clapeyron equation.

Table S3. Optimization table for the N-formylation reaction of N-methylaniline catalyzed by Co-COF.[a]

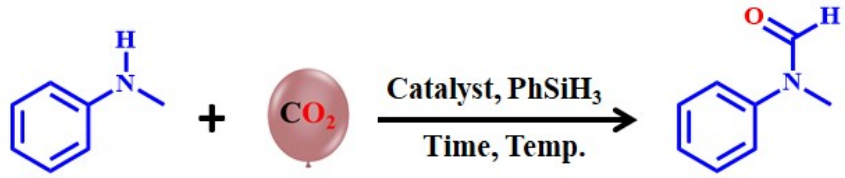

S. No.	Catalyst	Time (h)	Temperature (°C)	Yield (%)[b]
1	-	6	RT	-
2	EtDh-COF	6	RT	Trace
3	Co-COF	6	RT	51
4	Co-COF	9	RT	72
5	Co-COF	12	RT	96
6	Co-COF	9	50	55
7[c]	Co-COF	12	RT	73
8[d]	Co-COF	12	RT	62
9[e]	Co-COF	12	RT	84
10[f]	Co-COF	12	RT	36
11	$Co(OAc)_2.4H_2O$	12	RT	42
12[g]	Co-COF	12	RT	-
13[h]	Co-COF	12	RT	-
14[i]	Co-COF	12	RT	46

[a]**Reaction Conditions:** N-methylaniline (1 mmol), $PhSiH_3$ (2 mmol), catalyst (20 mg), dry DMF (2 mL), *b*: isolated yield, Solvents = [c]DMSO, [d]THF, [e]MeCN, *f*:$PhSiH_3$ (1 equiv.), *g*:under N_2, *h*:without $PhSiH_3$, *i*:catalyst (10 mg)

Catalytic Transformation of Amines to Formamides with Utilization of CO_2

N-formylation reaction of amines with CO_2 was carried out in a 30 ml Schlenk tube at RT (25 °C) under 1 atm CO_2 (balloon). Before the catalytic study, the catalyst was activated by treating it at 373 K under vacuum for 12 h. In a typical procedure, catalyst Co-COF (20 mg), amine (1 mmol), and $PhSiH_3$ (2 mmol) were taken in a Schlenk tube with 2 mL dry DMF. The CO_2 was introduced at 1 atm using a balloon, and the contents were stirred at RT for 12 h. After that, EtOAc was added to the mixture, and aqueous workup was performed. The combined organic phase was dried with anhydrous Na_2SO_4, and the product was purified by silica gel column chromatography using EtOAc/hexane (1:2) to give the corresponding formamides, and the obtained product was confirmed by both ^1H and ^{13}C NMR spectroscopy. The recovered catalyst was washed in dry acetone and methanol, then activated at 120 °C for 12 h under vacuum and reused for subsequent catalytic cycles.

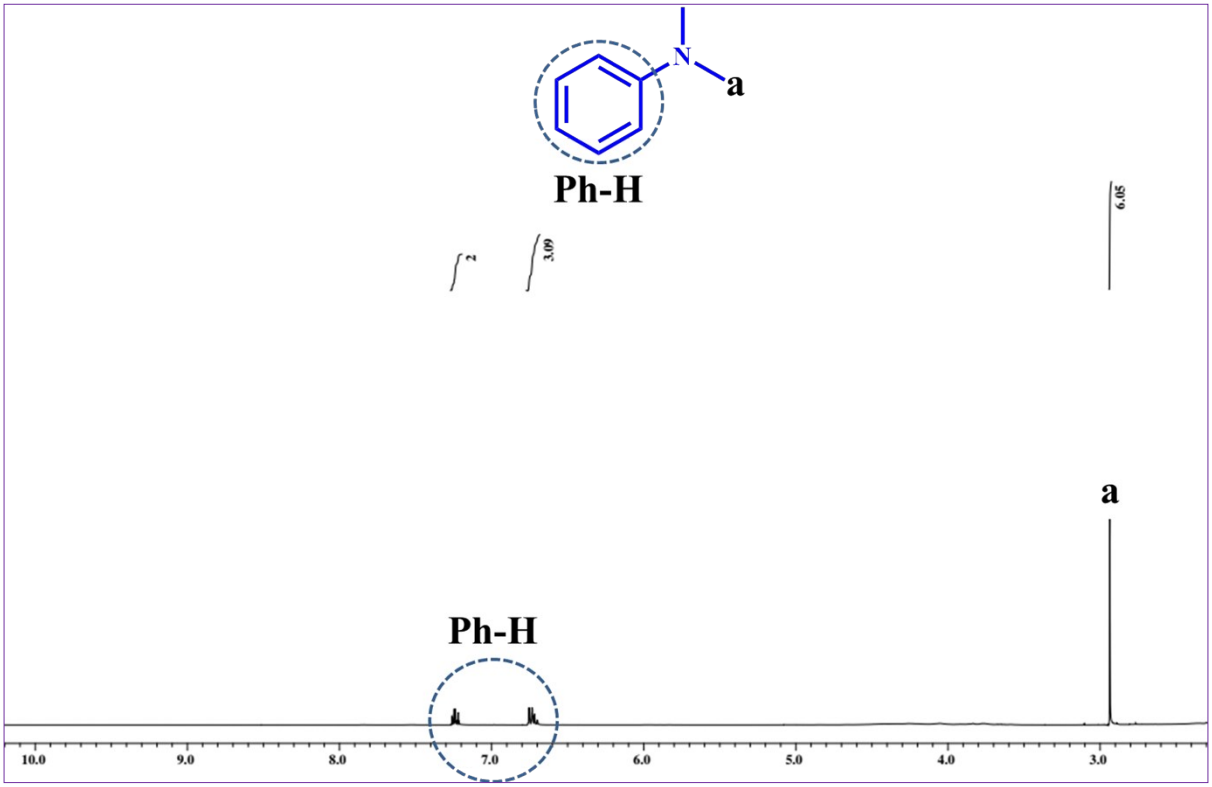

Figure S13. ^1H NMR ($CDCl_3$, 400 MHz) spectra of N,N-dimethylaniline catalyzed by Co-COF.

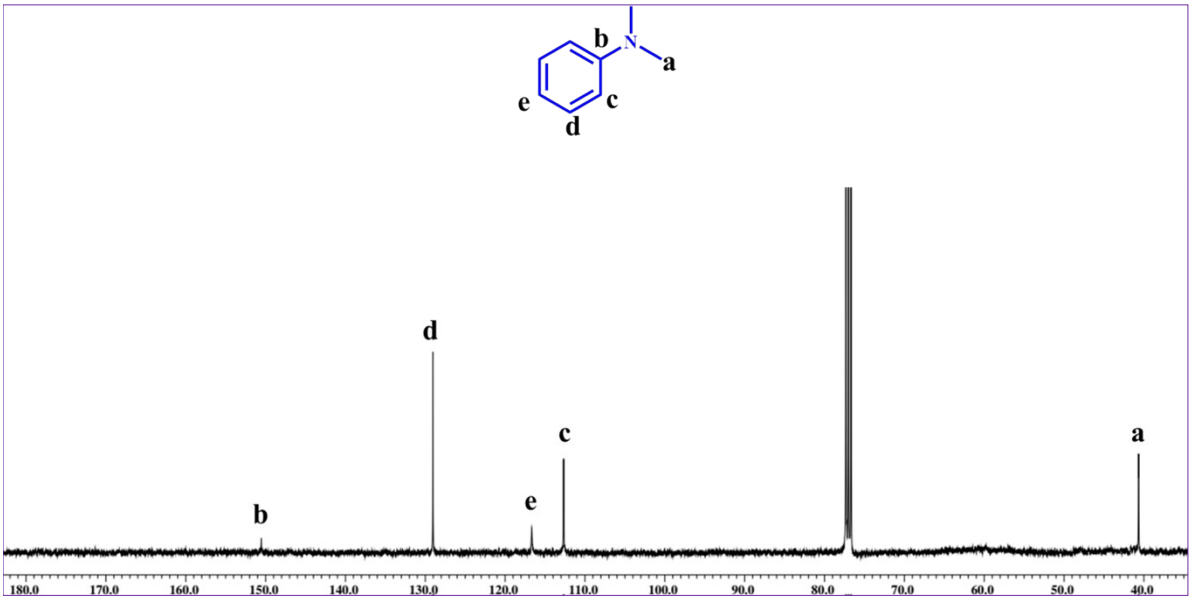

Figure S14. ^{13}C NMR ($CDCl_3$, 100 MHz) spectra of N,N-dimethylaniline catalyzed by Co-COF.

Table S4. ^{1}H and ^{13}C NMR data of N-formylated amine derivatives catalyzed by Co-COF under the optimized conditions.

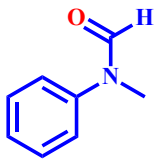	**N-methyl formanilide:** ^{1}H NMR (400 MHz, $CDCl_3$), δ (ppm): 8.45 (s, 1H), 7.37-7.41 (m, 2H), 7.25-7.27 (m, 1H), 7.14-7.16 (m, 2H), 3.30 (s, 3H). ^{13}C NMR (100 MHz, $CDCl_3$) δ (ppm): 32.07, 122.39, 126.41, 129.62, 142.25, 162.38.
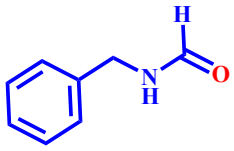	**N-benzyl formamide:** ^{1}H NMR (400 MHz, $CDCl_3$), δ (ppm): 8.14 (s, 1H), 7.19-7.35 (m, 5H), 6.59 (brs, 1H), 4.39 (d, 2H). ^{13}C NMR (100 MHz, $CDCl_3$), δ (ppm): 41.92, 126.82, 127.56, 128.57, 137.48, 161.20.
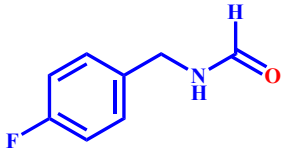	**N-(4-fluorobenzyl) formamide:** ^{1}H NMR (400 MHz, $CDCl_3$), δ (ppm): 8.24 (s, 1H), 7.27-7.22 (m, 2H), 7.02-6.98 (m, 2H), 5.89 (brs, 1H), 4.43 (d, 2H). ^{13}C NMR (100 MHz, $CDCl_3$), δ (ppm): 41.43, 115.62, 129.49, 133.35, 160.94, 163.45.
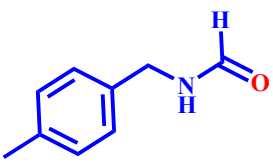	**N-(4-methylbenzyl) formamide:** ^{1}H NMR (400 MHz, $CDCl_3$), δ (ppm): 8.20 (s, 1H), 7.16-7.10 (m, 4H), 5.95 (brs, 1H), 4.40 (d, 2H), 2.31 (s, 3H). ^{13}C NMR (100 MHz, $CDCl_3$), δ (ppm): 21.05, 41.90, 127.76, 129.39, 134.47, 137.40, 160.92.

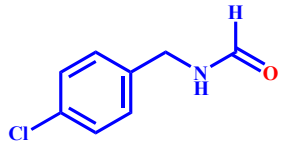	**N-(4-chlorobenzyl) formamide:** ^{1}H NMR (400 MHz, $CDCl_3$), δ (ppm): 8.19 (s, 1H), 7.28-7.22 (m, 2H), 7.16-7.11 (m, 2H), 5.97 (brs, 1H), 4.37 (d, 2H). ^{13}C NMR (100 MHz, $CDCl_3$), δ (ppm): 41.40, 128.85, 129.07, 133.45, 136.04, 161.01.
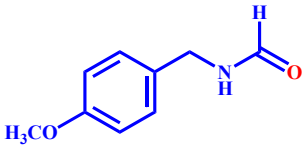	**N-(4-methoxybenzyl) formamide:** ^{1}H NMR (400 MHz, $CDCl_3$), δ (ppm): 8.22 (s, 1H), 7.21 (d, 2H), 6.87 (d, 2H), 5.93 (brs, 1H), 4.41 (d, 2H), 3.79 (s, 3H). ^{13}C NMR (100 MHz, $CDCl_3$), δ (ppm): 41.61, 55.26, 114.15, 128.26, 129.16, 159.07, 160.87.
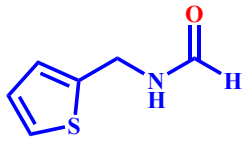	**N-(thiophen-2-yl) formamide:** ^{1}H NMR (400 MHz, $CDCl_3$), δ (ppm): 8.17 (s, 1H), 7.23- 7.19 (m, 1H), 6.98-6.91 (m, 2H), 6.41 (brs, 1H), 4.61 (d, 2H). ^{13}C NMR (100 MHz, $CDCl_3$), δ (ppm): 36.76, 125.36, 126.25, 126.92, 139.98, 160.78.
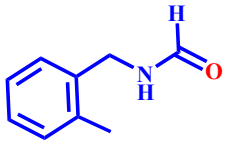	**N-(2-methylbenzyl)formamide:** ^{1}H NMR (400 MHz, $CDCl_3$), δ (ppm): 8.21 (s, 1H), 7.25- 7.15 (m, 4H), 6.11 (brs, 1H), 4.45 (d, 2H), 2.32 (s, 3H). ^{13}C NMR (100 MHz, $CDCl_3$), δ (ppm): 18.9, 40.16, 126.16, 127.95, 128.12, 130.81, 135.11, 136.42, 161.15.
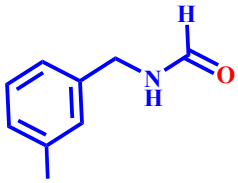	**N-(3-methylbenzyl)formamide:** ^{1}H NMR (400 MHz, $CDCl_3$), δ (ppm): 8.19 (s, 1H), 7.22 (t, 1H), 7.19-7.01 (m, 3H), 6.79 (brs, 1H), 4.39 (d, 2H), 2.31 (s, 3H). ^{13}C NMR (100 MHz, $CDCl_3$), δ (ppm): 21.11, 41.91, 127.96, 128.55, 128.92, 137.28, 138.11, 161.72.

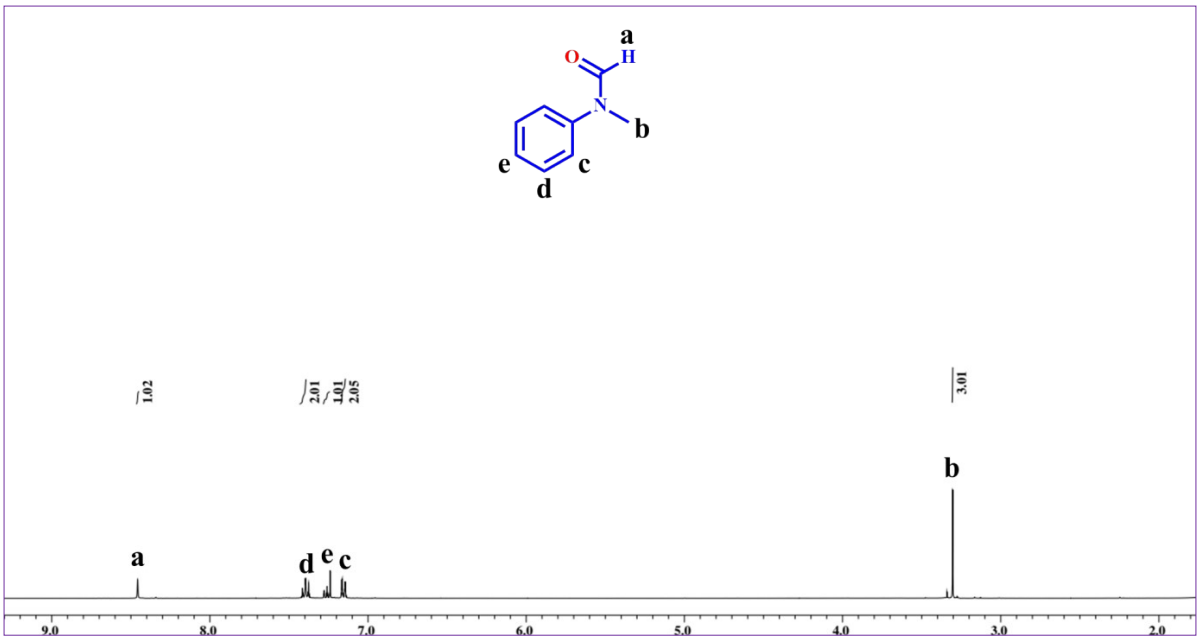

Figure S15. ^{1}H NMR ($CDCl_3$, 400 MHz) spectra of N-methylformanilide catalyzed by Co-COF under the optimized conditions.

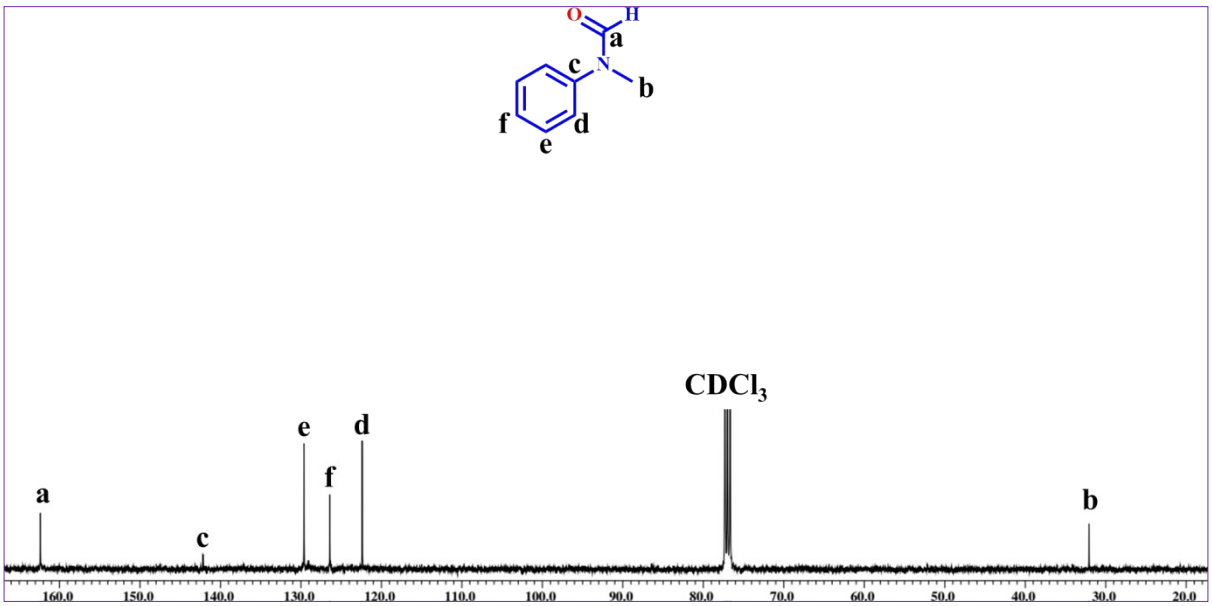

Figure S16. ^{13}C NMR ($CDCl_3$, 100 MHz) spectra of N-methylformanilide catalyzed by Co-COF under the optimized conditions.

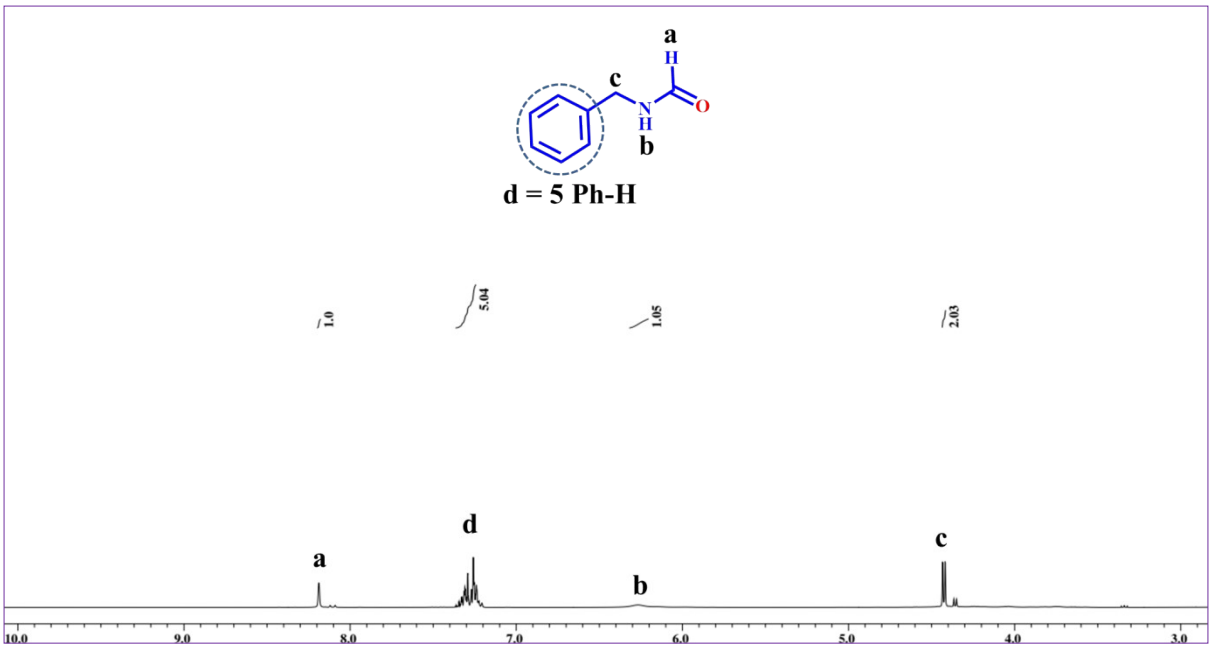

Figure S17. ^{1}H NMR ($CDCl_3$, 400 MHz) spectra of N-benzyl formamide catalyzed by Co-COF under the optimized conditions.

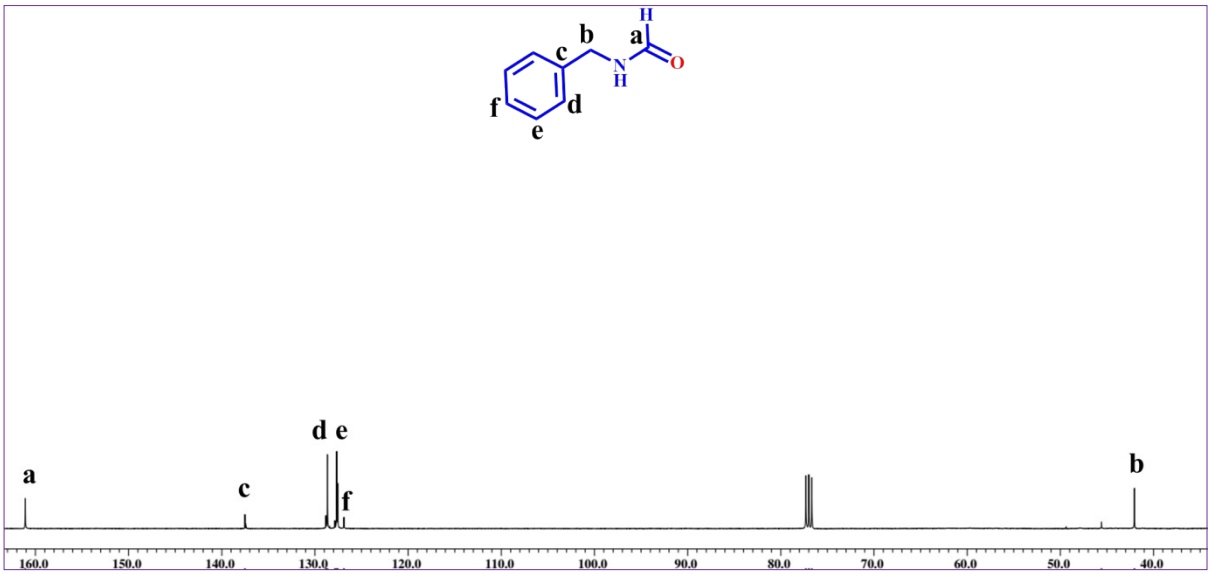

Figure S18. ^{13}C NMR ($CDCl_3$, 100 MHz) spectra of N-benzyl formamide catalyzed by Co-COF under the optimized conditions.

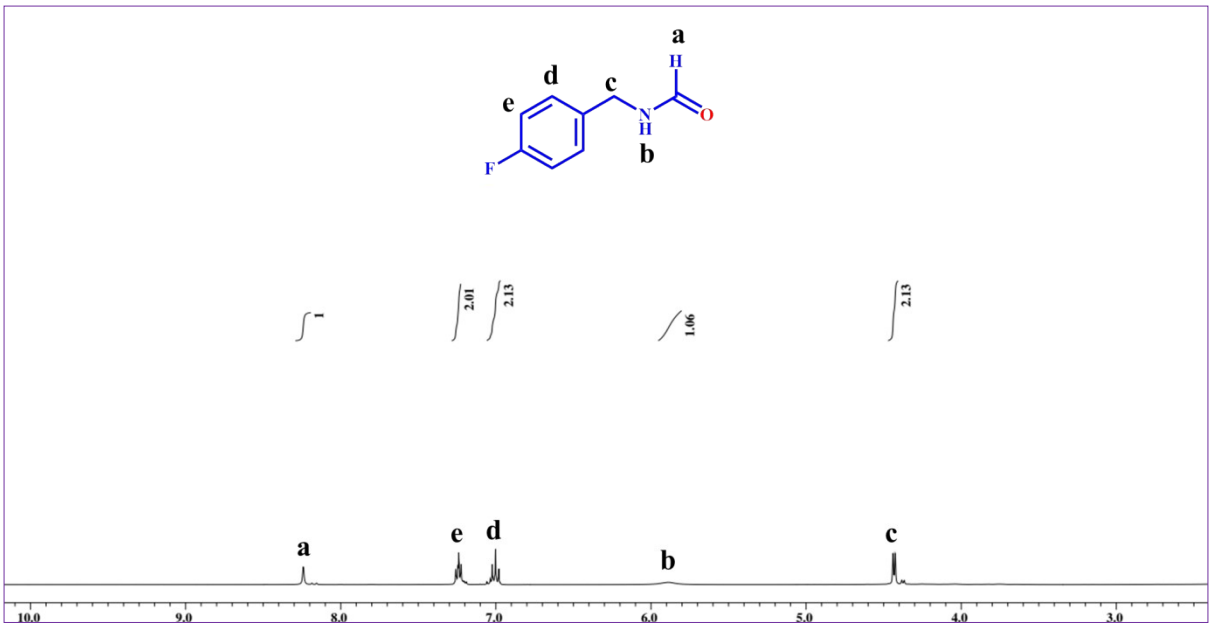

Figure S19. ^{1}H NMR ($CDCl_3$, 400 MHz) spectra of N-(4-fluorobenzyl) formamide catalyzed by Co-COF under the optimized conditions.

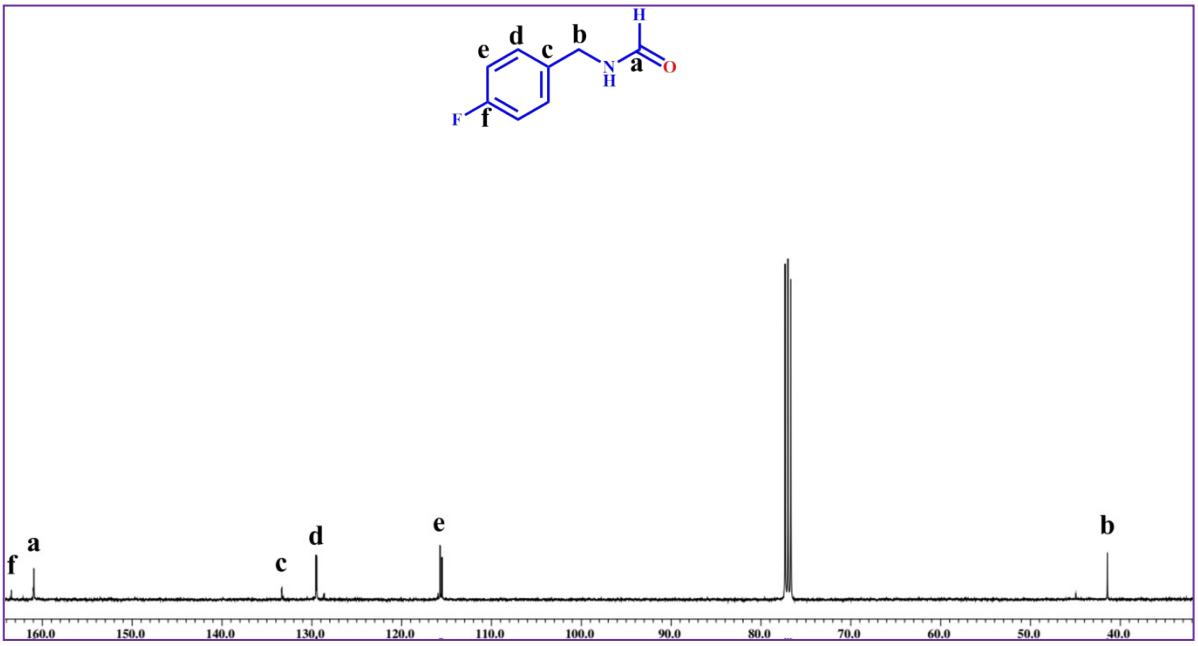

Figure S20. ^{13}C NMR ($CDCl_3$, 100 MHz) spectra of N-(4-fluorobenzyl) formamide catalyzed by Co-COF under the optimized conditions.

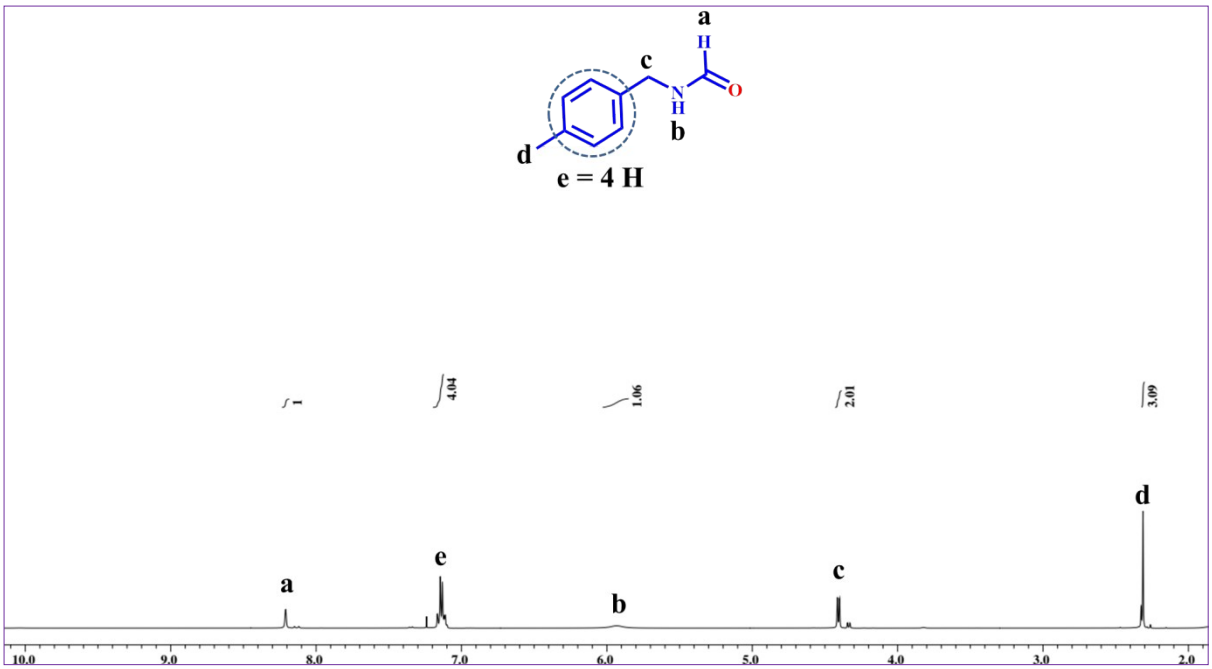

Figure S21. ^{1}H NMR ($CDCl_3$, 400 MHz) spectra of N-(4-methylbenzyl) formamide catalyzed by Co-COF under the optimized conditions.

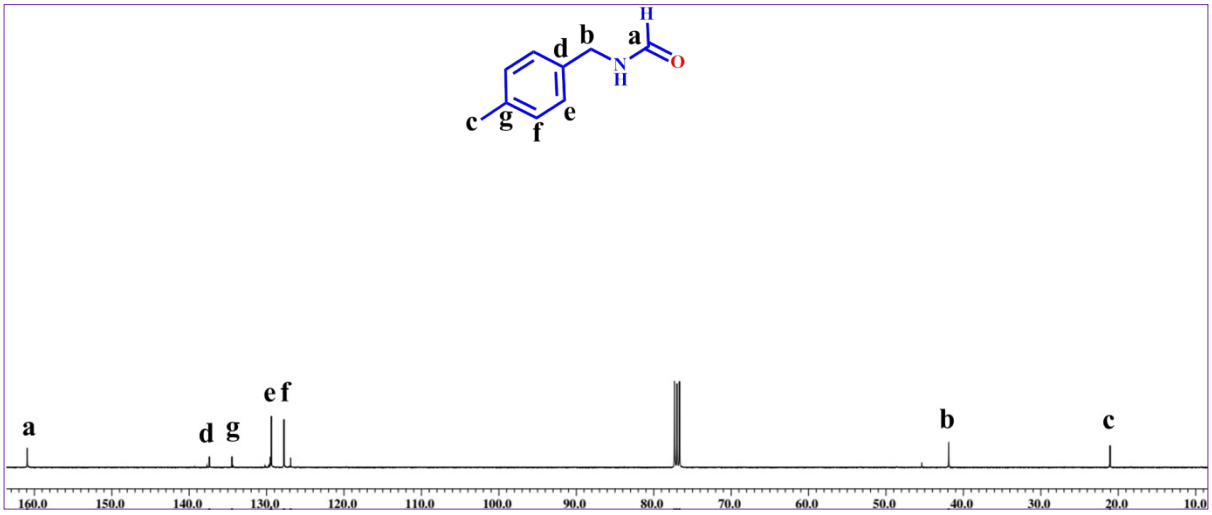

Figure S22. ^{13}C NMR ($CDCl_3$, 100 MHz) spectra of N-(4-methylbenzyl) formamide catalyzed by Co-COF under the optimized conditions.

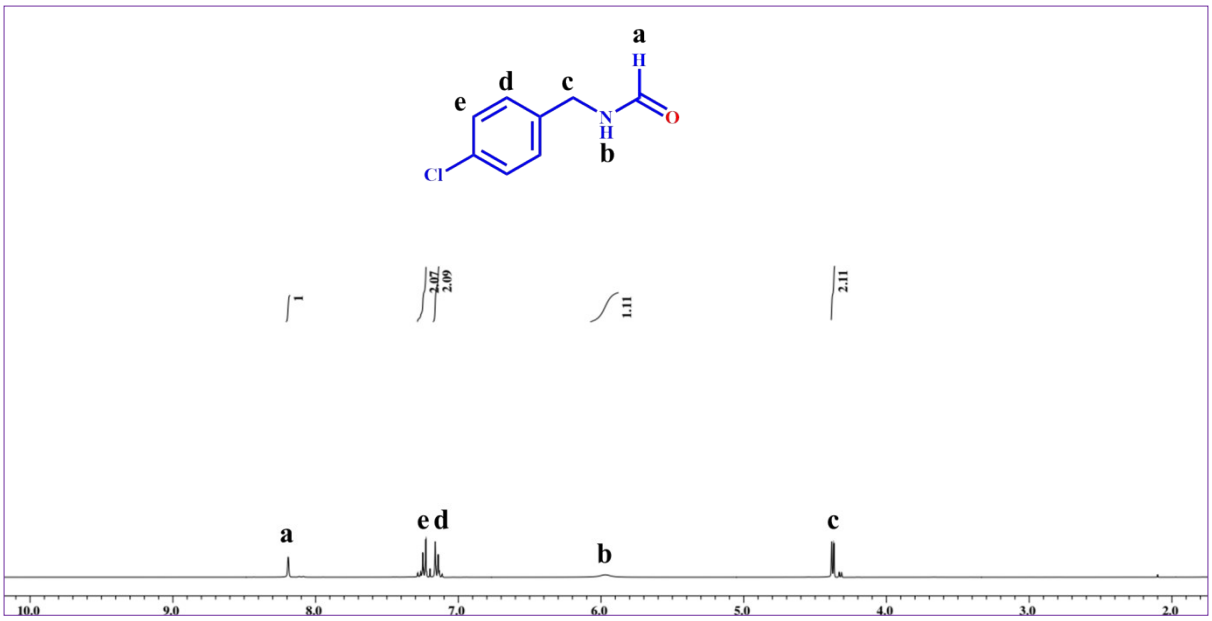

Figure S23. ^{1}H NMR ($CDCl_3$, 400 MHz) spectra of N-(4-chlorobenzyl) formamide catalyzed by Co-COF under the optimized conditions.

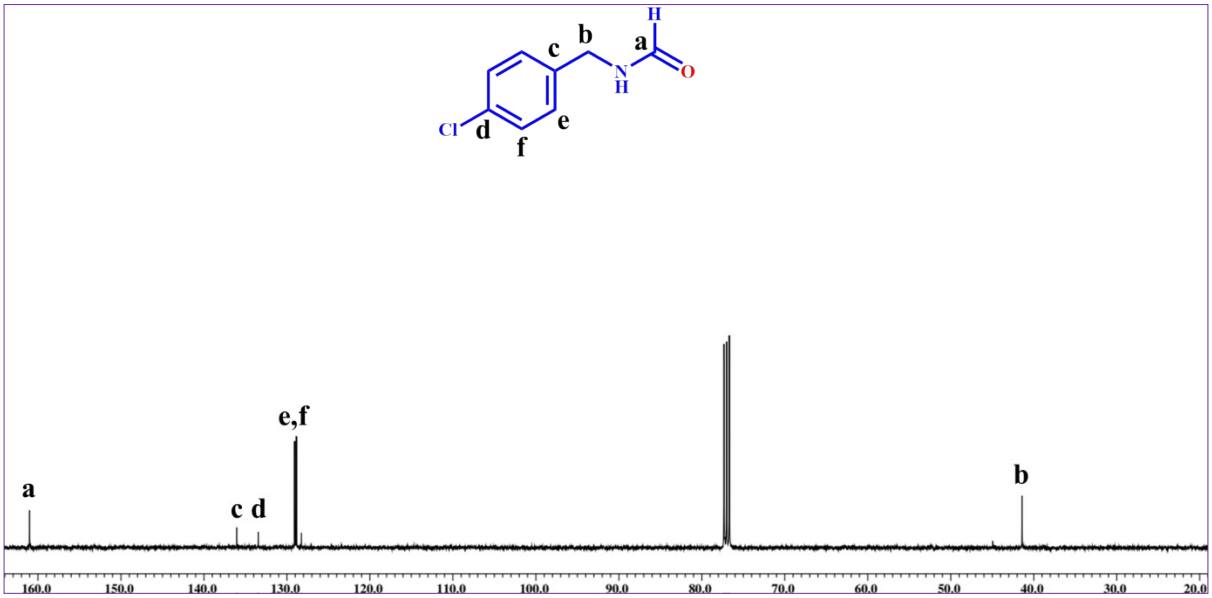

Figure S24. ^{13}C NMR ($CDCl_3$, 100 MHz) spectra of N-(4-chlorobenzyl) formamide catalyzed by Co-COF under the optimized conditions.

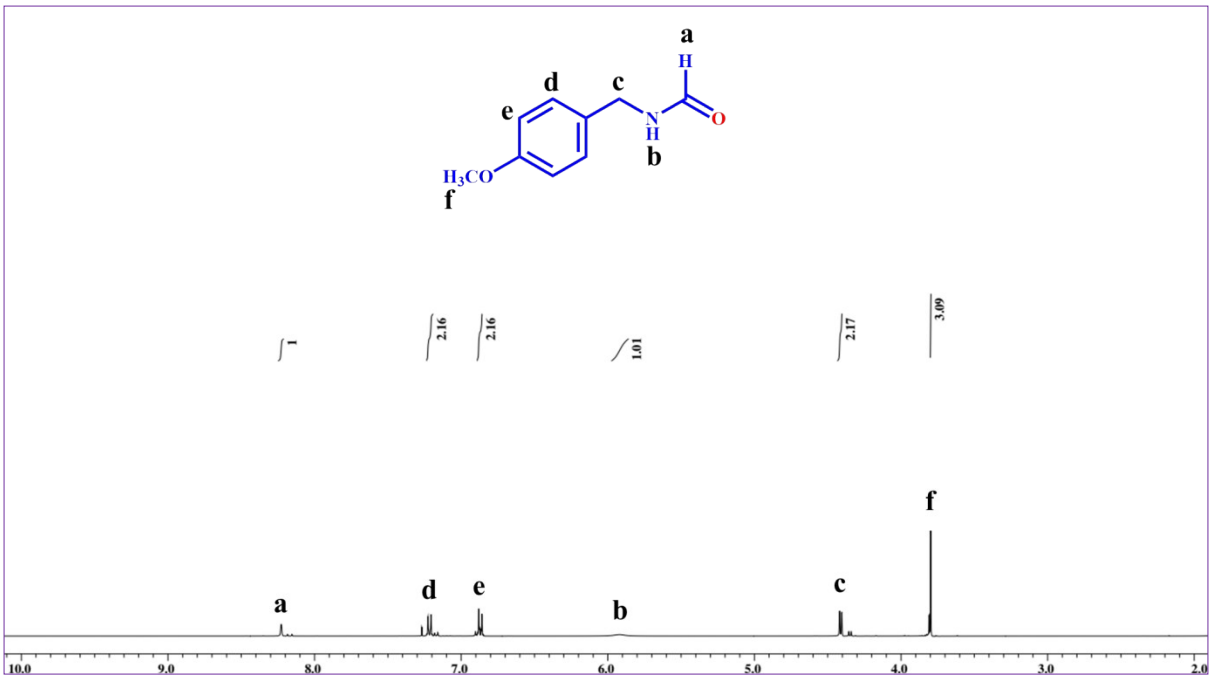

Figure S25. ^{1}H NMR ($CDCl_3$, 400 MHz) spectra of N-(4-methoxybenzyl) formamide catalyzed by Co-COF under the optimized conditions.

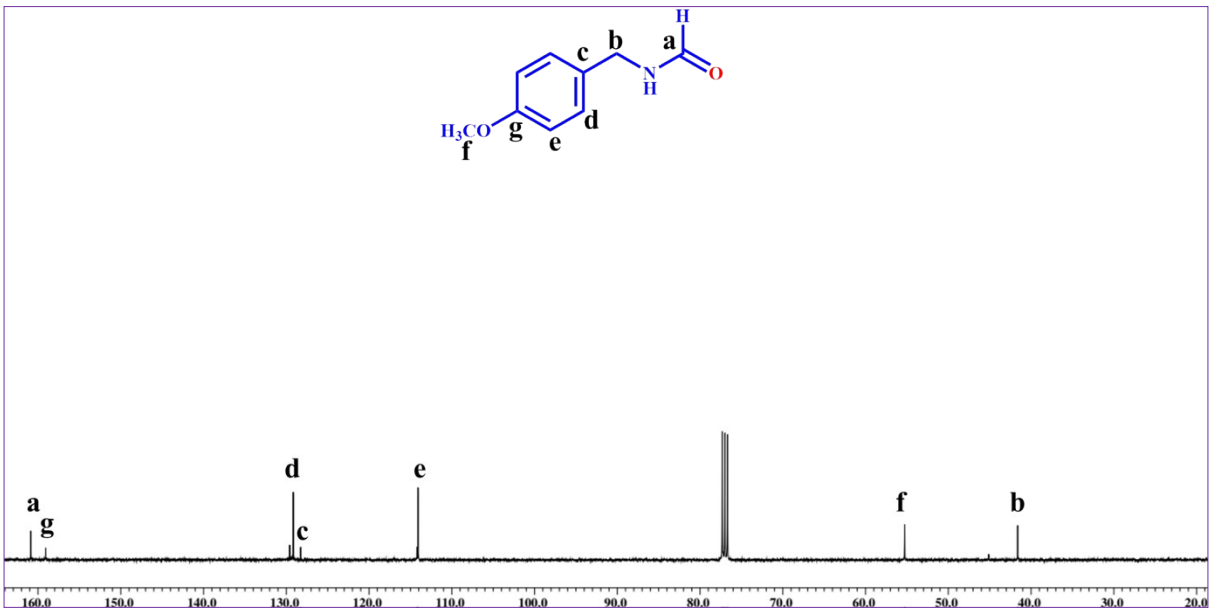

Figure S26. ^{13}C NMR ($CDCl_3$, 100 MHz) spectra of N-(4-methoxybenzyl) formamide catalyzed by Co-COF under the optimized conditions.

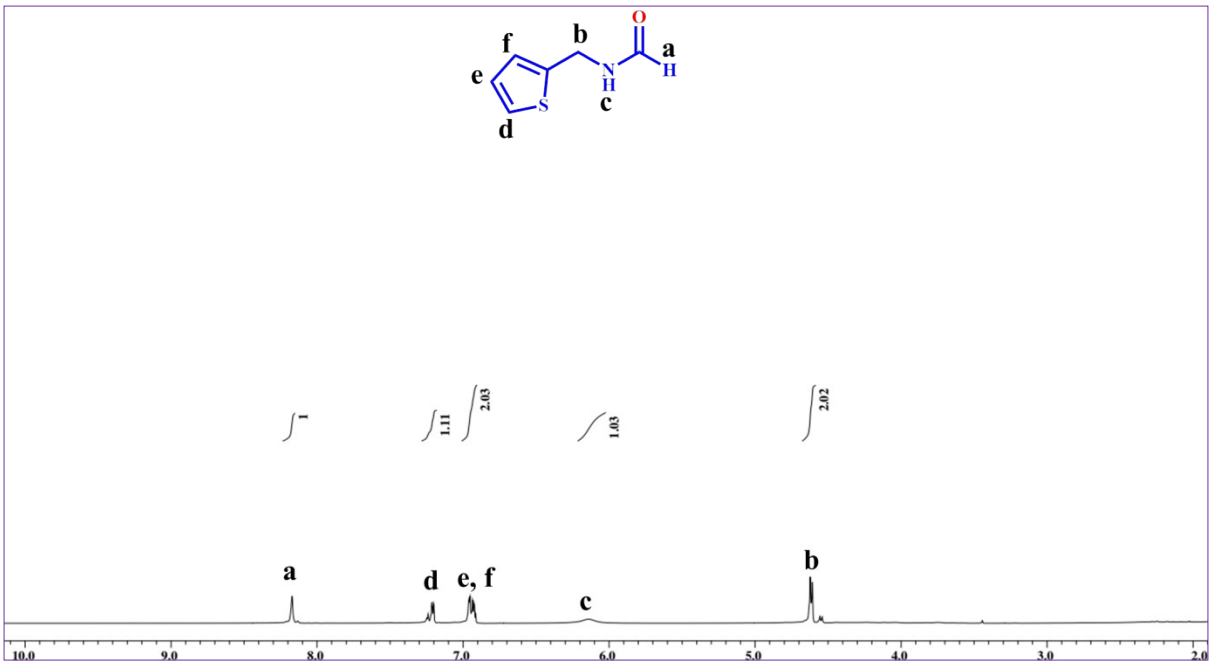

Figure S27. ^{1}H NMR ($CDCl_3$, 400 MHz) spectra of N-(thiophen-2-yl) formamide catalyzed by Co-COF under the optimized conditions.

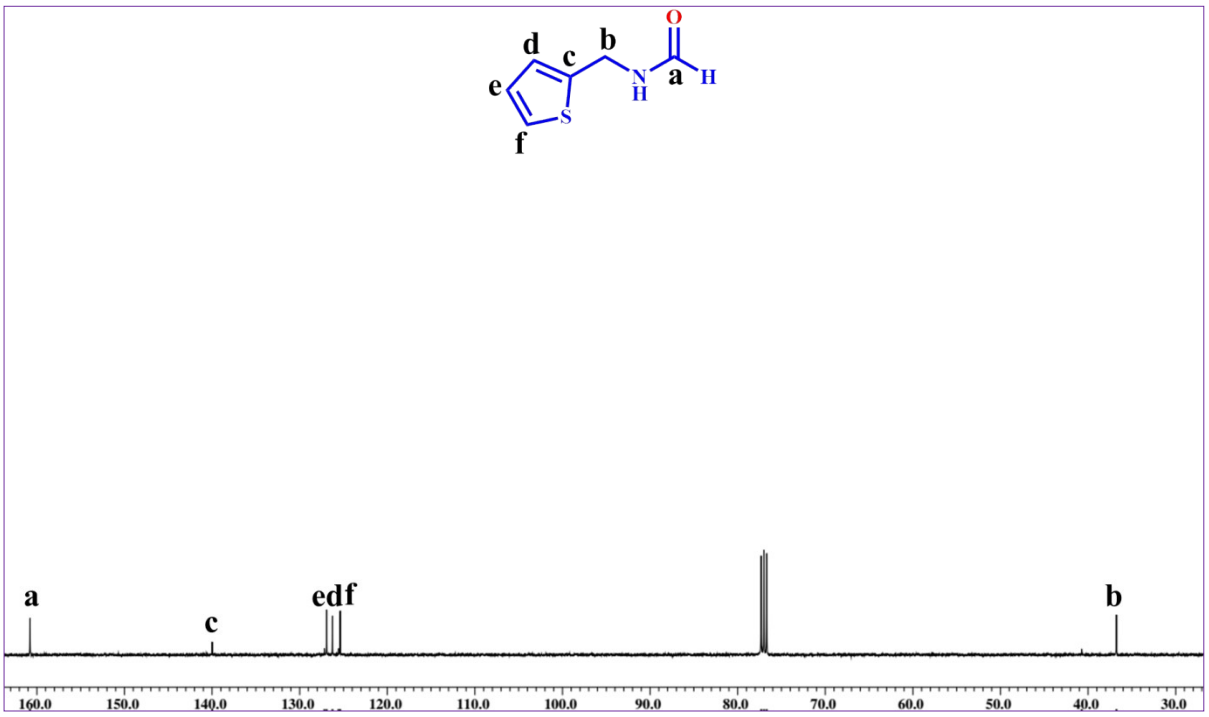

Figure S28. ^{13}C NMR ($CDCl_3$, 100 MHz) spectra of N-(thiophen-2-yl) formamide catalyzed by Co-COF under the optimized conditions.

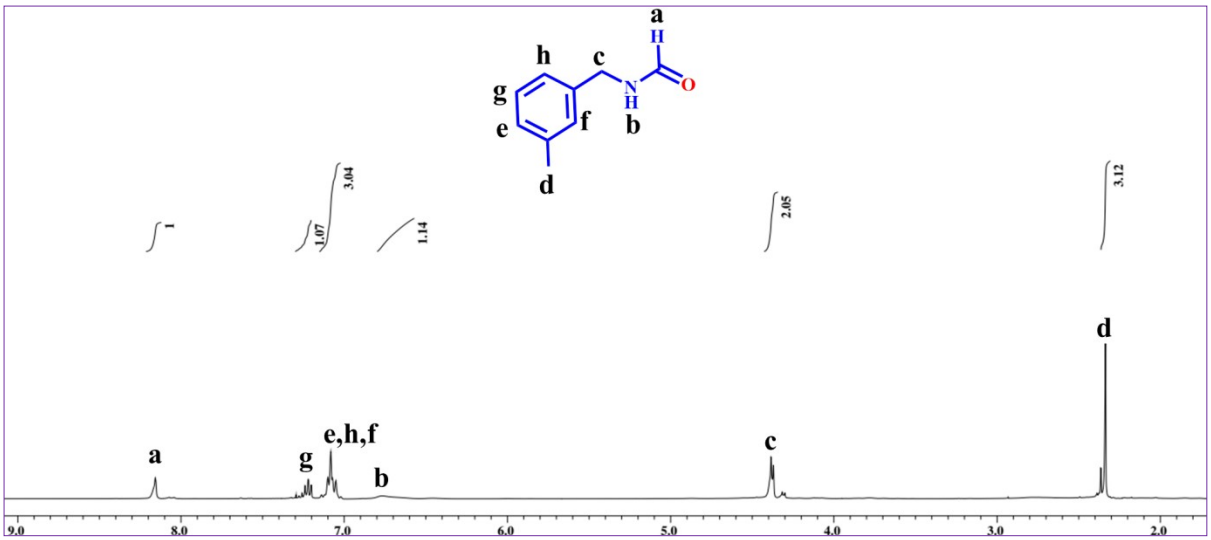

Figure S29. ^{1}H NMR ($CDCl_3$, 400 MHz) spectra of N-(3-methylbenzyl)formamide catalyzed by Co-COF under the optimized conditions.

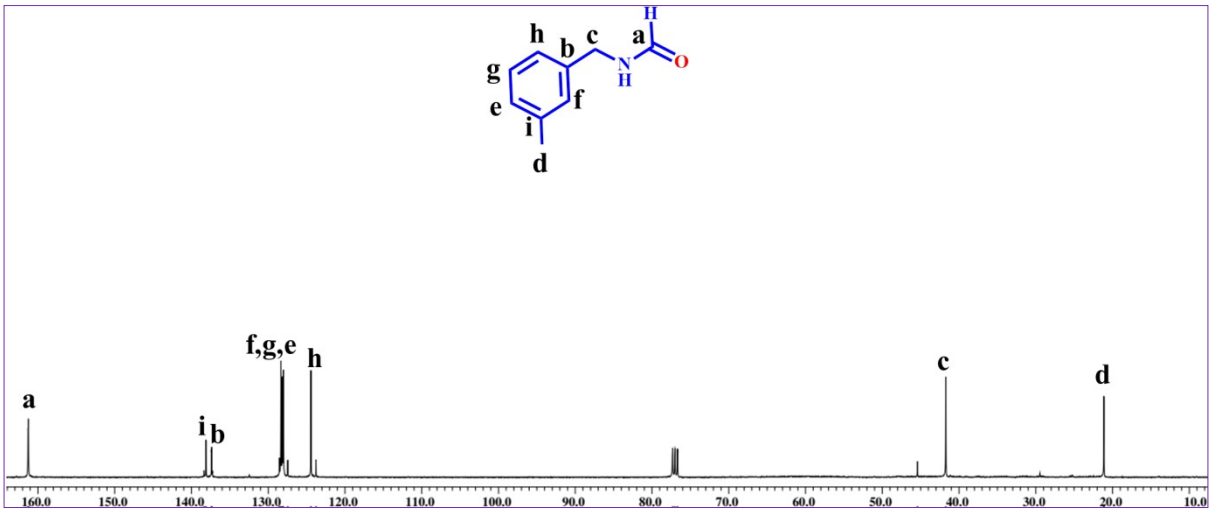

Figure S30. ^{13}C NMR ($CDCl_3$, 100 MHz) spectra of N-(3-methylbenzyl)formamide catalyzed by Co-COF under the optimized conditions.

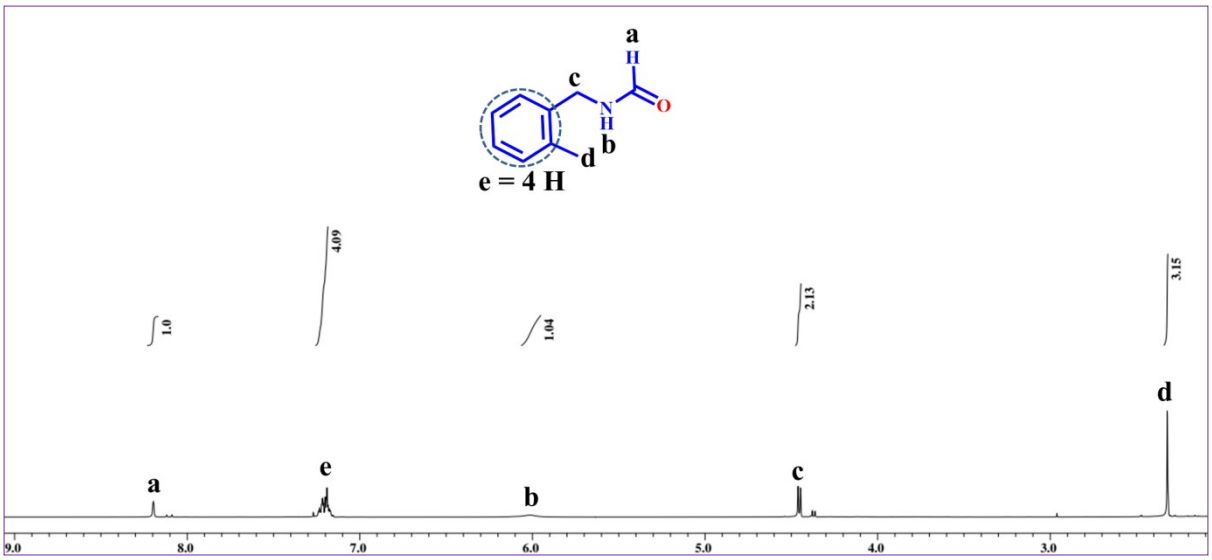

Figure S31. ^{1}H NMR ($CDCl_3$, 400 MHz) spectra of N-(2-methylbenzyl)formamide catalyzed by Co-COF under the optimized conditions.

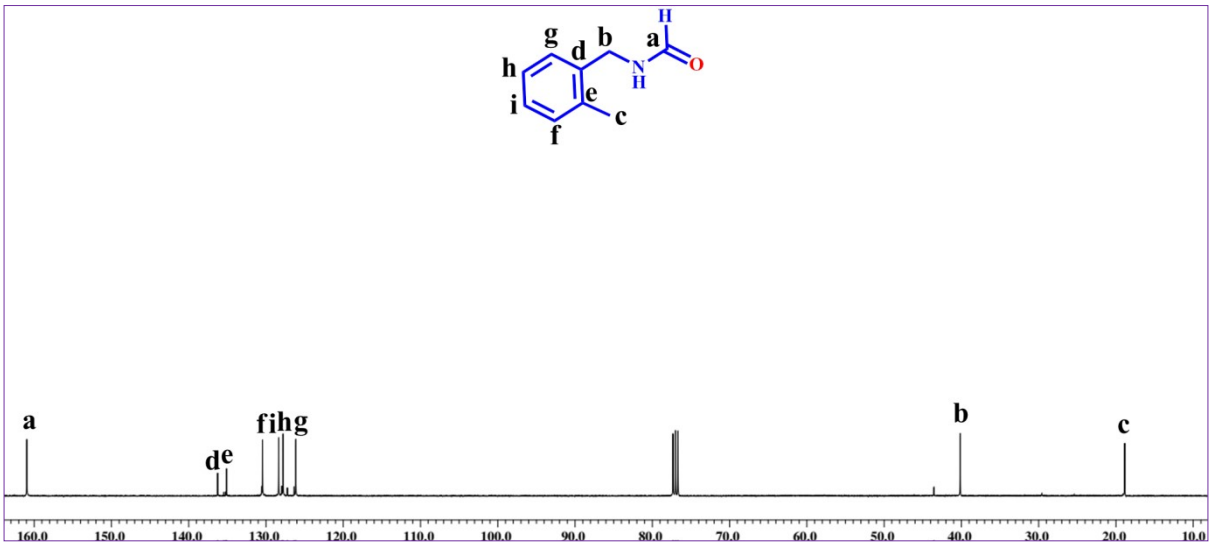

Figure S32. ^{13}C NMR ($CDCl_3$, 100 MHz) spectra of N-(2-methylbenzyl)formamide catalyzed by Co-COF under the optimized conditions.

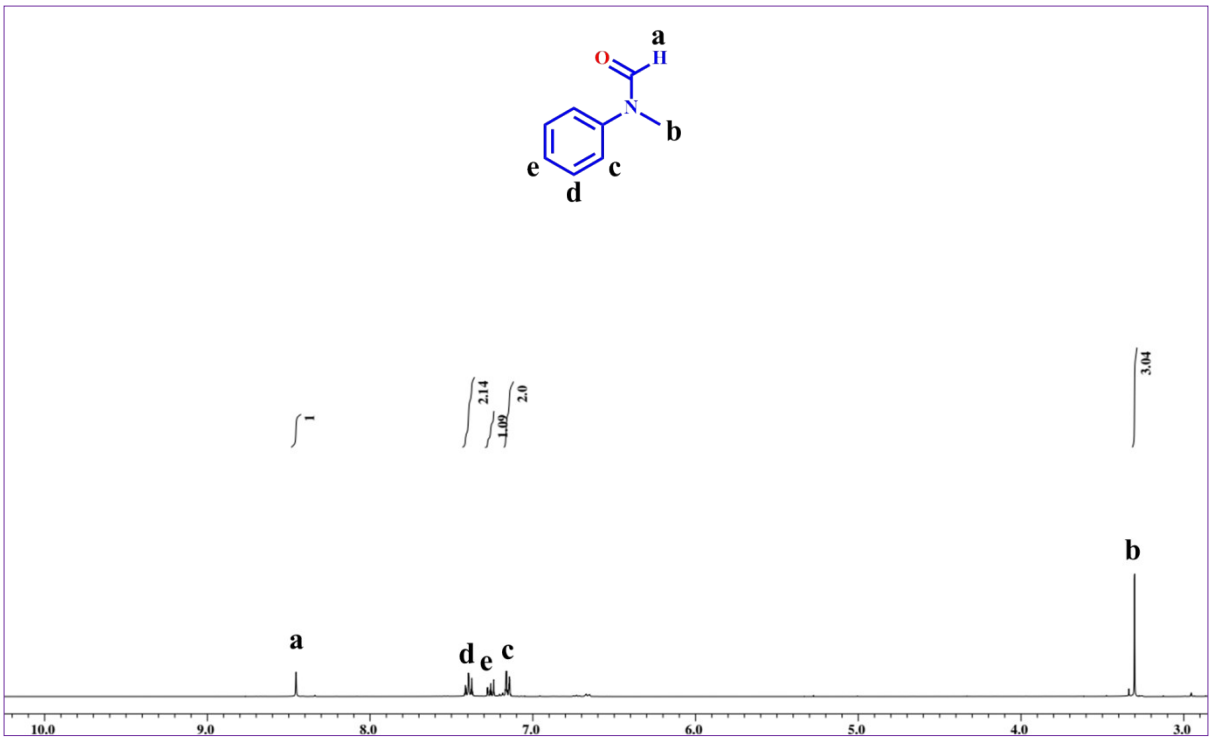

Figure S33. ^{1}H NMR ($CDCl_3$, 400 MHz) spectra of N-methylformanilide catalyzed by Co-COF under the optimized conditions using simulated flue gas (13:87% = CO_2:N_2) under the optimized conditions.

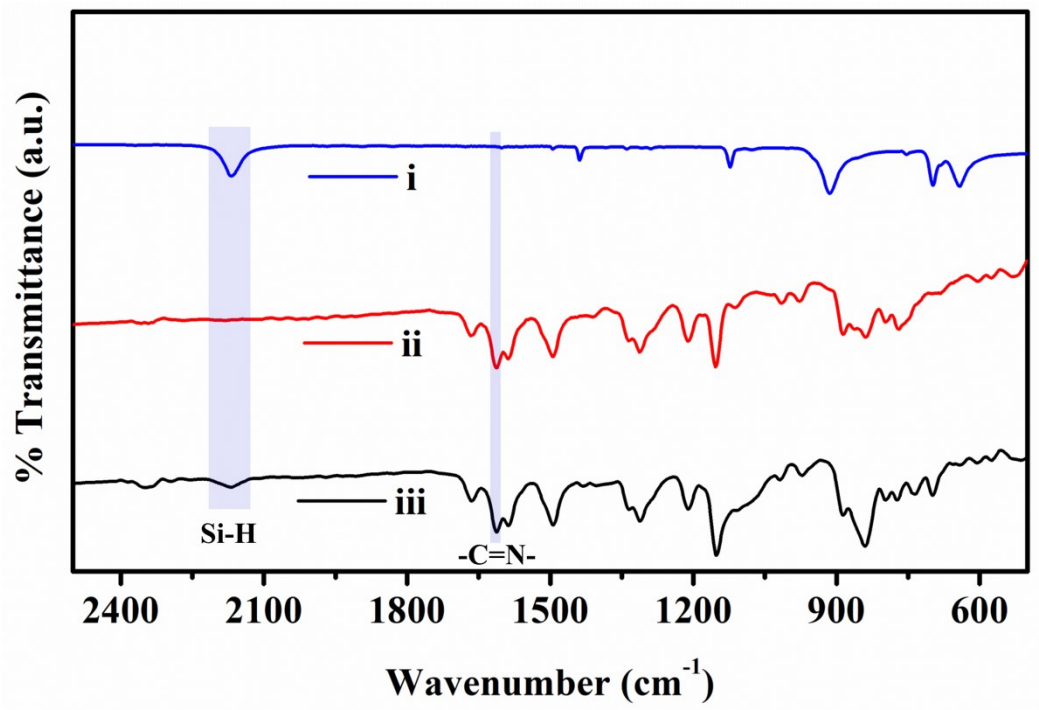

Figure S34. FT-IR spectra of (i) $PhSiH_3$, (ii) EtDh-COF treated with $PhSiH_3$, (iii) Co-COF treated with $PhSiH_3$.

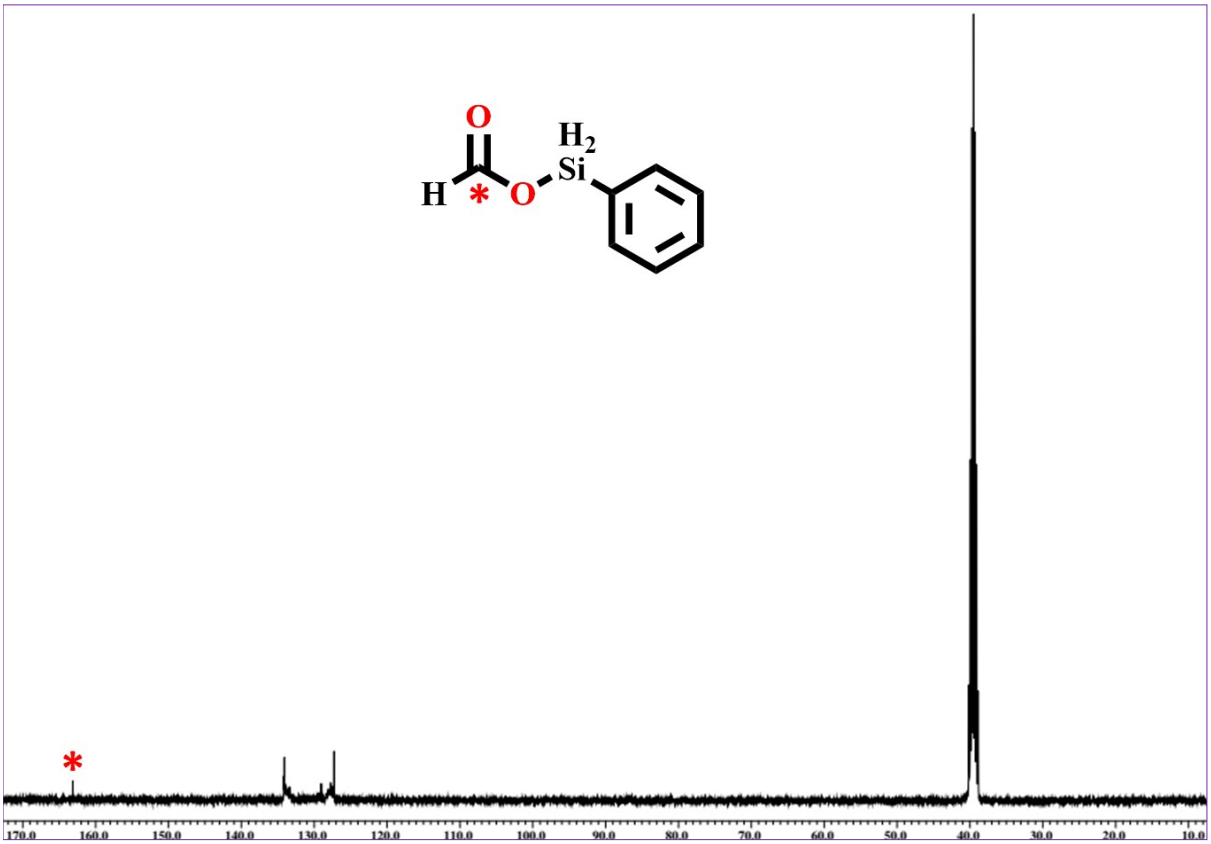

Figure S35. ^{13}C NMR (DMSO-D_6, 100 MHz) spectra of formoxysilane catalyzed by Co-COF.

Table S5. Comparison of the catalytic activity of Co-COF with the reported heterogeneous catalysts for the N-formylation reaction of N-methylaniline using hydrosilanes as a reducing agent.

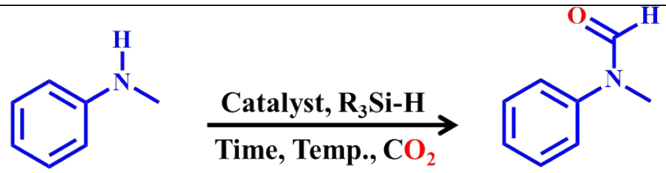

Sl. No.	Catalyst	Time (h)	Temp. (°C)	Yield (%)	Ref.
1	Co_2@MIL-101(Cr)	24	25	94	4
2	Au@Ir-PCN-222	24	25	90	5
3	$[Et_4NBr]_{50\%}$-Py-COF	24	30	94	6
4	Ni-MOF	12	RT	95	7
5	Zn-TpPa	18	30	99.99	8
6	CAU-10pydc	12	RT	90	9
7	**Co-COF**	**12**	**RT**	**96**	**This work**

Synthesis of propargylic amines

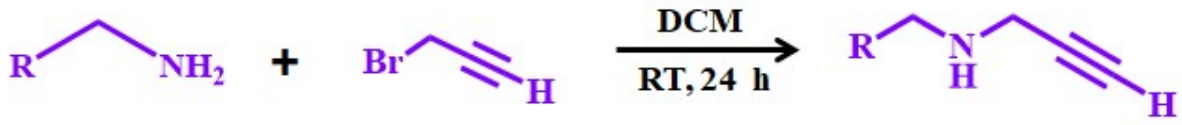

Scheme S1. The general method for the synthesis of various propargylic amines.

In a typical procedure, propargylic bromide (2.7 mmol) was slowly added into a 50 mL round-bottom flask containing amine (16.2 mmol) within 30 min in the presence of 20 mL DCM. Subsequently, the resulting mixture was stirred at room temperature for 24 hours. After that, the solvent was removed under vacuum, and the obtained mixture was diluted with ether and washed with a saturated aqueous solution of $NaHCO_3$ (3×10 mL). The organic phase was dried over anhydrous Na_2SO_4, and the reaction mixture was purified by silica gel column chromatography to afford the corresponding product.

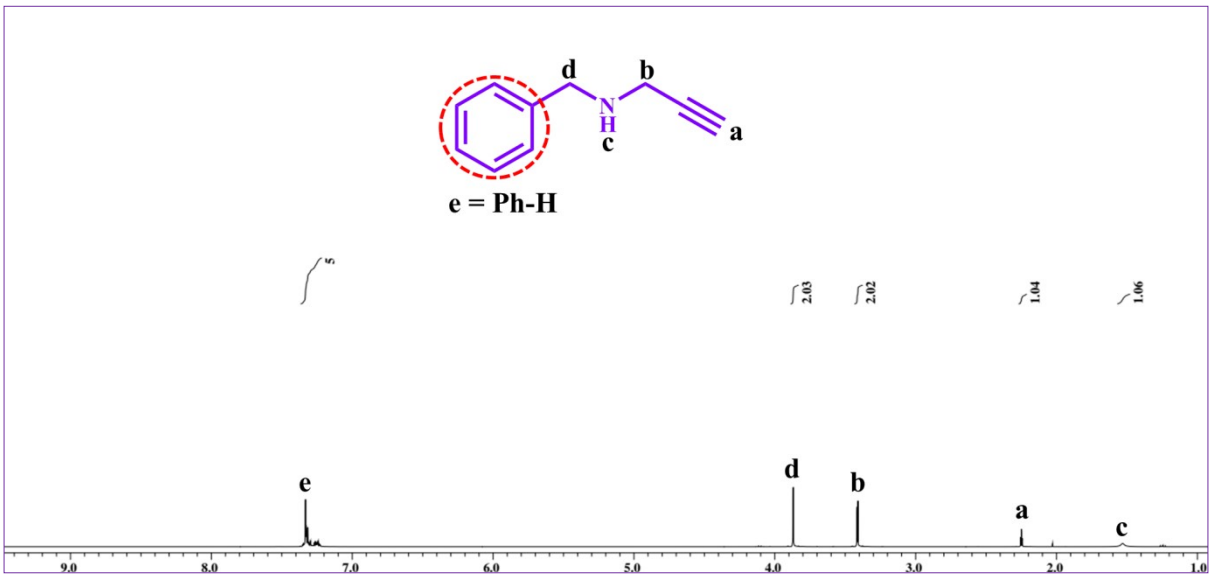

Figure S36. ^1H NMR ($CDCl_3$, 400 MHz) spectra of N-benzylprop-2-yn-1-amine.

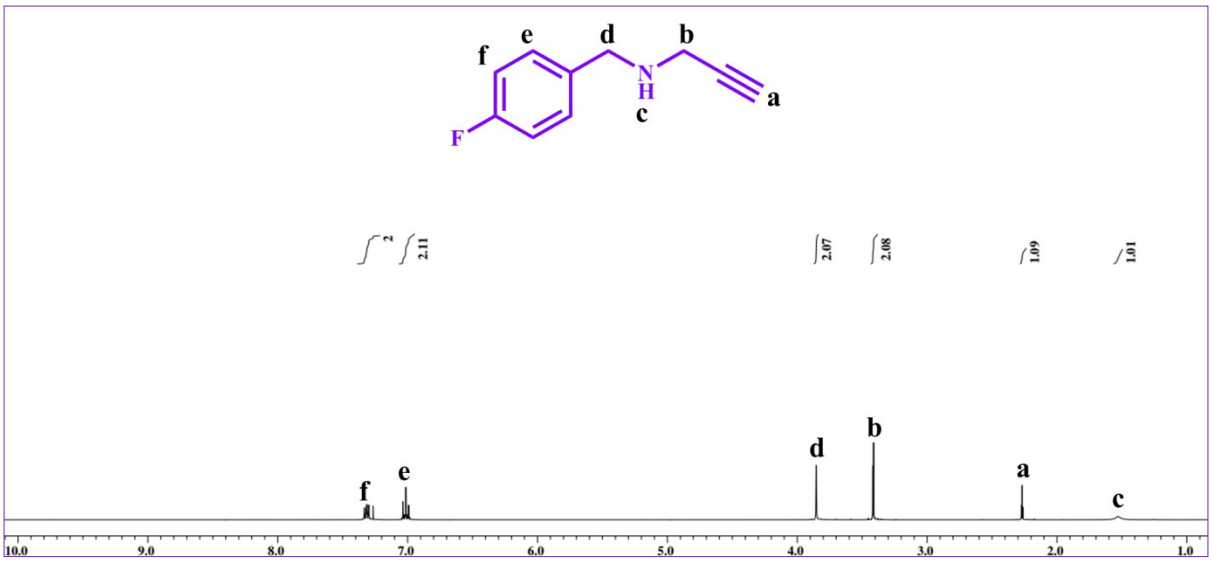

Figure S37.[1]H NMR ($CDCl_3$, 400 MHz) spectra of N-(4-fluorobenzyl)prop-2-yn-1-amine.

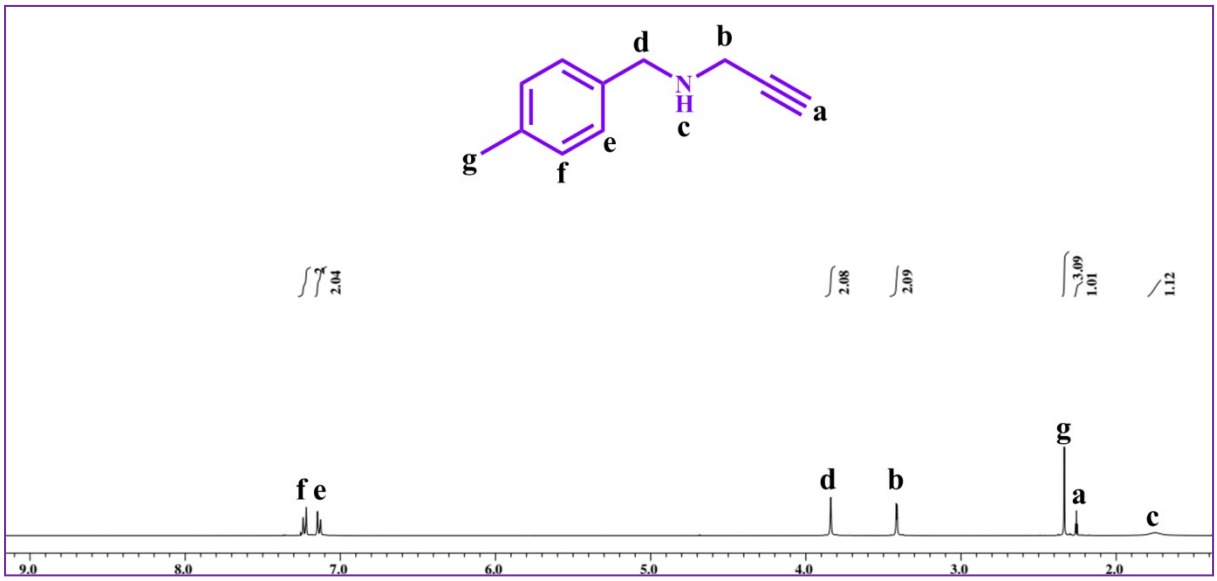

Figure S38. [1]H NMR ($CDCl_3$, 400 MHz) spectra of N-(4-methylbenzyl)prop-2-yn-1-amine.

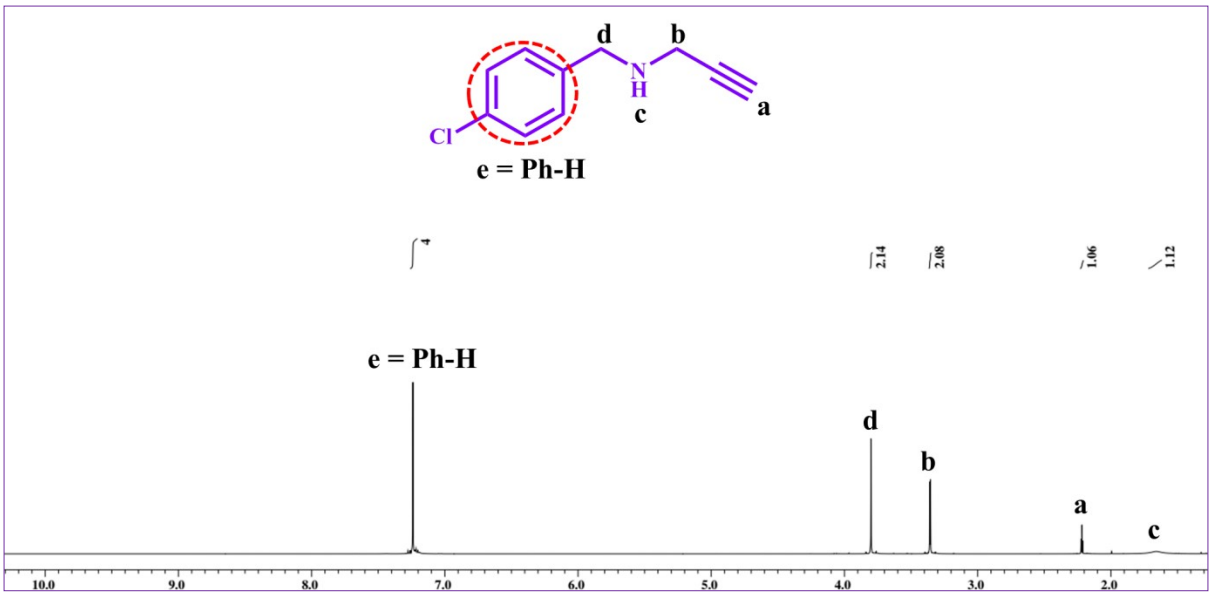

Figure S39. ^{1}H NMR ($CDCl_3$, 400 MHz) spectra of N-(4-chlorobenzyl)prop-2-yn-1-amine.

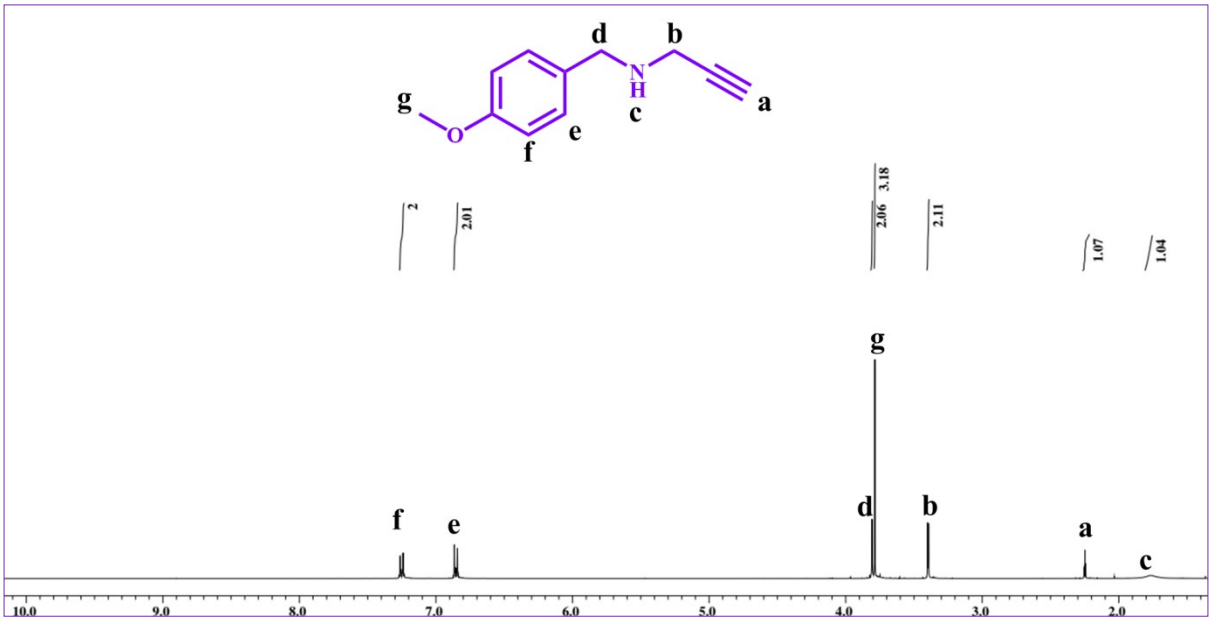

Figure S40. ^{1}H NMR ($CDCl_3$, 400 MHz) spectra of N-(4-methoxybenzyl)prop-2-yn-1-amine.

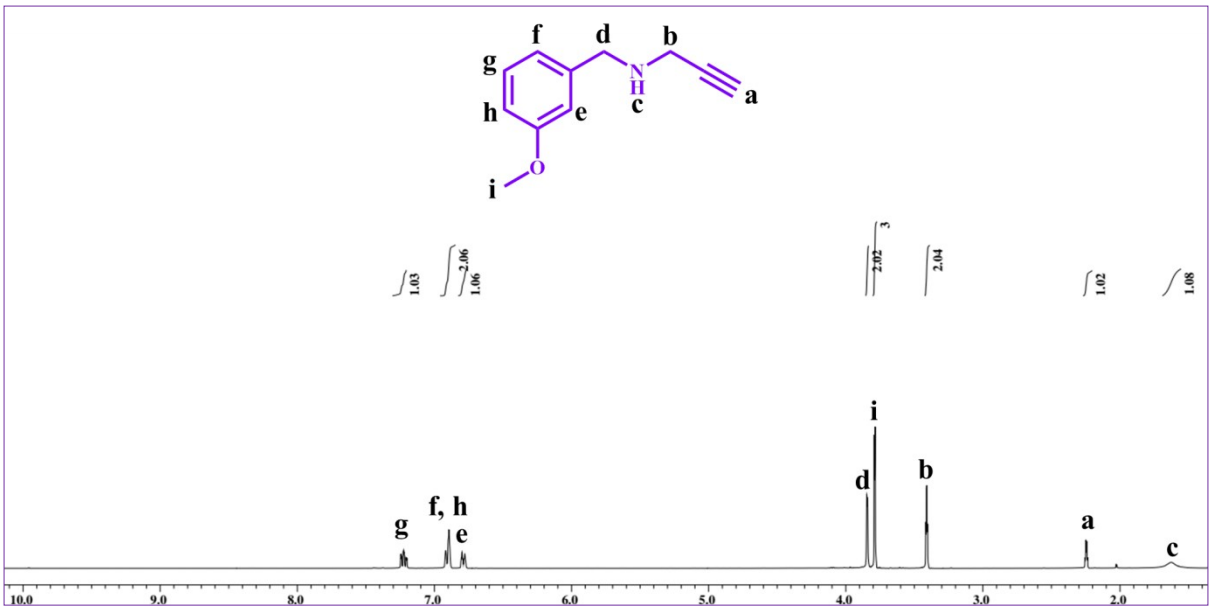

Figure S41. ^{1}H NMR ($CDCl_3$, 400 MHz) spectrum of N-(3-methoxybenzyl)prop-2-yn-1-amine.

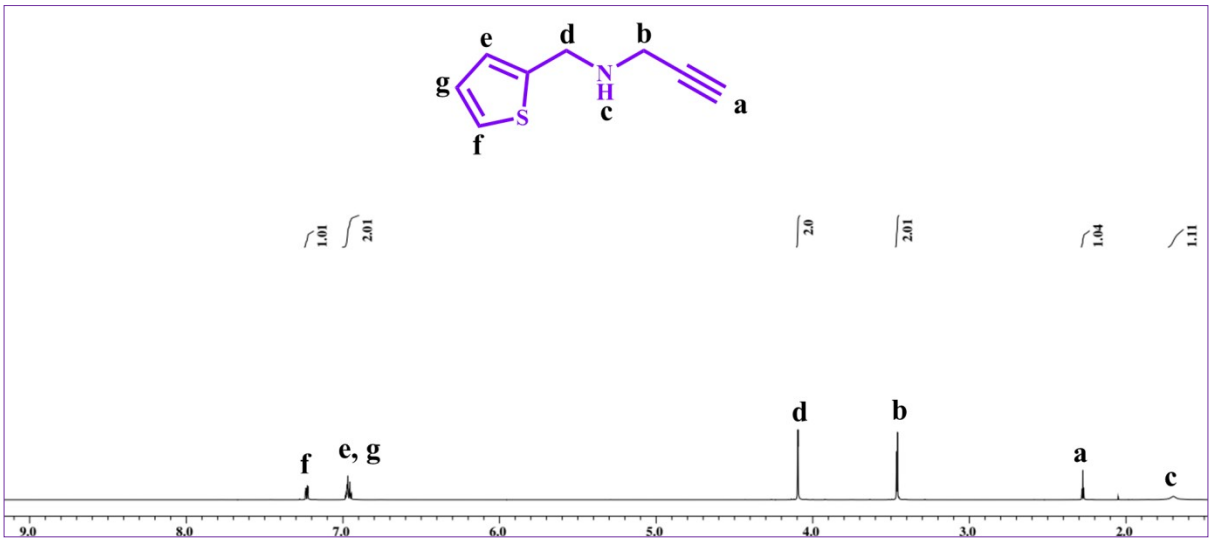

Figure S42. ^{1}H NMR ($CDCl_3$, 400 MHz) spectra of N-(thiophen-2-ylmethyl)prop-2-yn-1-amine.

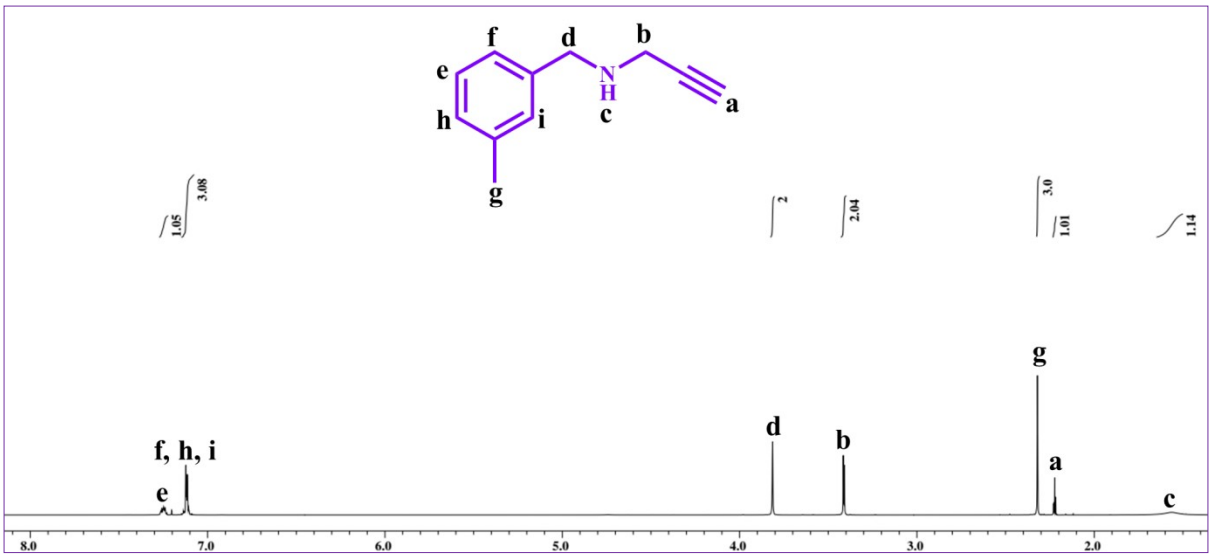

Figure S43. ^{1}H NMR ($CDCl_3$, 400 MHz) spectra of N-(3-methylbenzyl)prop-2-yn-1-amine.

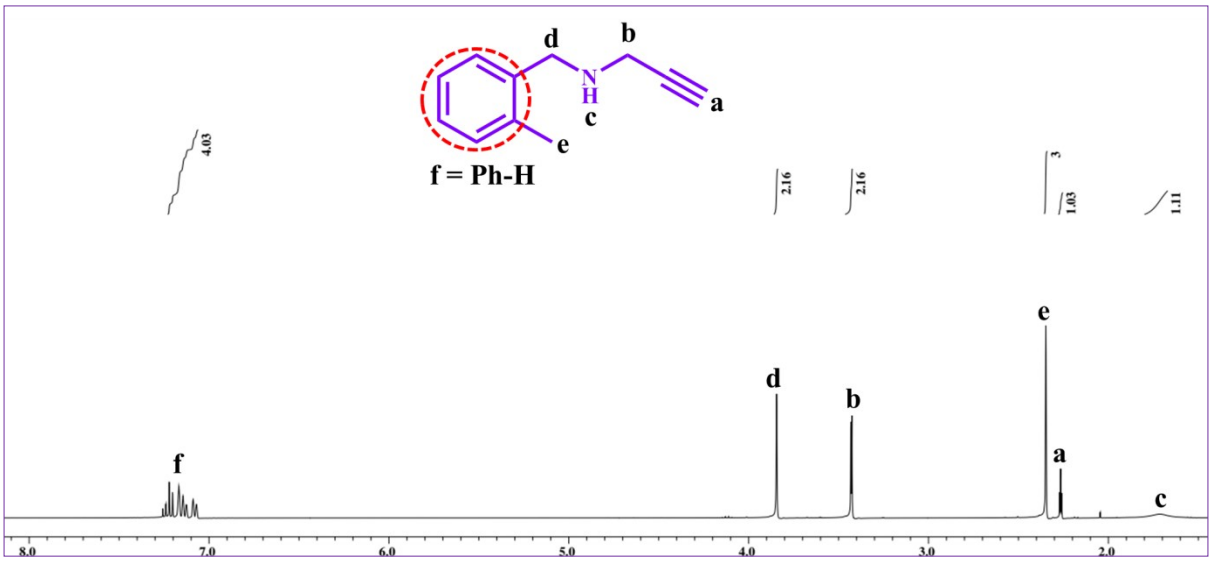

Figure S44. ^{1}H NMR ($CDCl_3$, 400 MHz) spectra of N-(2-methylbenzyl)prop-2-yn-1-amine.

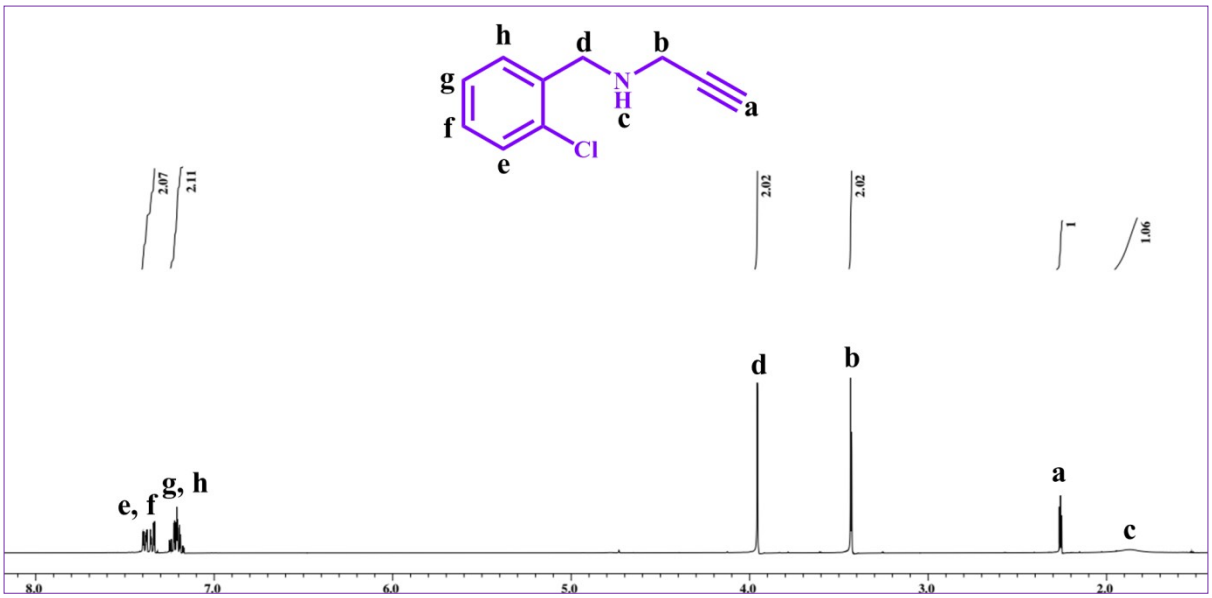

Figure S45. ^{1}H NMR ($CDCl_3$, 400 MHz) spectra of N-(2-chlorobenzyl)prop-2-yn-1-amine.

Table S6. Optimization table for the carboxylative cyclization of N-benzylprop-2-yn-1-amine.[a]

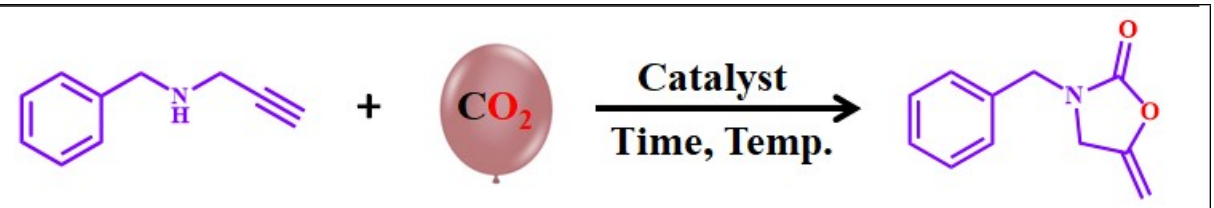

S. No.	Catalyst	Time (h)	Temperature (°C)	Yield (%)[b]
1	-	6	RT	-
2	EtDh-COF	6	RT	-
4	Co-COF	6	RT	38
5	Co-COF	6	40	52
6	Co-COF	9	40	74
7	Co-COF	12	40	99
8	$Co(OAc)_2 \cdot 4H_2O$	12	40	47
9[c]	Co-COF	12	40	76
10[d]	Co-COF	12	40	87
11[e]	Co-COF	12	40	48
12[f]	Co-COF	12	40	trace
13[g]	Co-COF	12	40	-

[a]**Reaction Conditions:** N-benzylprop-2-yn-1-amine (1 mmol), catalyst (20 mg), DBU (0.1 equiv), DMSO (2 mL), *b*: the percentage yield was determined by ^{1}H NMR analysis, [c]DMF, [d]MeCN, [e]catalyst (10 mg), *f*: without DBU, *g*: under N_2

Catalytic Conversion of Propargylic Amines to 2-Oxazolidinones with Utilization of CO_2

The catalytic cyclic carboxylation of propargylic amines was carried out in a 30 ml Schlenk tube at 40 °C under 1 atm CO_2 (balloon). Before the catalytic experiments, the catalyst was activated by treating it at 373 K under vacuum for 12 h. In a typical procedure, catalyst Co-COF (20 mg), propargylic amine (1 mmol), and DBU (0.1 equiv.) were taken in a Schlenk tube with 2 mL DMSO. The CO_2 was introduced at 1 atm using a balloon, and the contents were stirred at 40 °C for 12 h. After that, the catalyst was separated by centrifugation, and diethyl ether was added to the mixture, and aqueous workup was performed. The combined organic phase was dried with anhydrous Na_2SO_4, and the solvent was removed under vacuum to get the desired product. The obtained product was confirmed by both ^{1}H and ^{13}C NMR spectroscopy. The recovered catalyst was washed in dry acetone and methanol, then activated at 100 °C for 12 h under vacuum and reused for subsequent catalytic cycles.

Table S7. ^{1}H and ^{13}C NMR data of 2-oxazolidinone derivatives catalyzed by Co-COF under the optimized conditions.

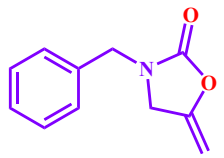	**3-benzyl-5-methyleneoxazolidin-2-one:** ^{1}H NMR (400 MHz, $CDCl_3$), δ (ppm): 7.35-7.25 (m, 5H), 4.71-4.69 (q, 1H), 4.39 (s, 2H), 4.22-4.20 (q, 1H), 3.99 (t, 2H). ^{13}C NMR (100 MHz, $CDCl_3$), δ (ppm): 155.59, 148.85, 134.87, 128.90, 128.19, 128.10, 86.73, 47.75, 47.14.
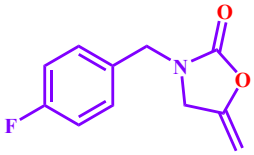	**3-(4-fluorobenzyl)-5methyleneoxazolidin-2-one:** ^{1}H NMR (400 MHz, $CDCl_3$), δ (ppm): 7.26-7.22 (m, 2H), 7.06-7.02 (m, 2H), 4.75-4.73 (q, 1H), 4.42 (s, 2H), 4.25-4.23 (q, 1H), 3.99 (t, 2H). ^{13}C NMR (100 MHz, $CDCl_3$), δ (ppm): 163.78, 161.32, 155.55, 148.69, 130.73, 129.93, 129.85, 115.98, 115.76, 86.95, 47.10.
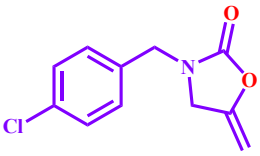	**3-(4-chlorobenzyl)-5methyleneoxazolidin-2-one:** ^{1}H NMR (400 MHz, $CDCl_3$), δ (ppm): 7.32-7.29 (m, 2H), 7.20-7.17 (m, 2H), 4.74-4.71 (q, 1H), 4.41 (s, 2H), 4.24-4.22 (m, 1H), 3.99 (t, 2H). ^{13}C NMR (100 MHz, $CDCl_3$), δ (ppm): 155.57, 148.61, 134.15, 133.44, 129.47, 129.13, 87.09, 47.13.
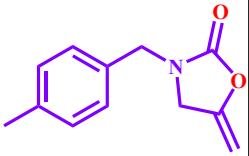	**3-(4-methylbenzyl)-5methyleneoxazolidin-2-one:** ^{1}H NMR (400 MHz, $CDCl_3$), δ (ppm): 7.14 (s, 4H), 4.71-4.70 (q, 1H), 4.40 (s, 2H), 4.20-4.19 (q, 1H), 3.97 (t, 2H), 2.32 (s, 3H). ^{13}C NMR (100 MHz, $CDCl_3$), δ (ppm): 155.58, 148.95, 138.04, 131.83, 129.58, 128.16, 86.66, 47.52, 47.09, 21.10.
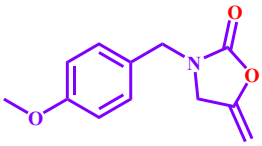	**3-(4-methoxybenzyl)-5methyleneoxazolidin-2-one:** ^{1}H NMR (400 MHz, $CDCl_3$), δ (ppm): 7.27 (d, 2H), 6.86 (d, 2H), 4.71-4.70 (q, 1H), 4.38 (s, 2H), 4.20-4.19 (q, 1H), 3.78 (s, 3H). ^{13}C NMR (100 MHz, $CDCl_3$), δ (ppm): 159.55, 155.45, 148.96, 129.58, 126.92, 114.26, 86.67, 55.28, 47.22, 47.04.
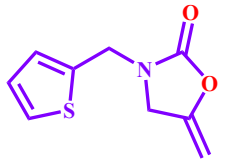	**5-methylene-3-(thiophen-3-ylmethyl)oxazolidin-2-one:** ^{1}H NMR (400 MHz, $CDCl_3$), δ (ppm): 7.28-7.26 (m, 1H), 7.01-6.95 (m, 2H), 4.73-4.71 (q, 1H), 4.63 (s, 2H), 4.25-4.23 (q, 1H), 4.08 (t, 2H). ^{13}C NMR (100 MHz, $CDCl_3$), δ (ppm): 155.21, 148.72, 136.99, 127.45, 127.15, 126.27, 86.99, 47.03, 42.17.
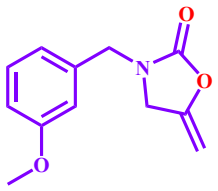	**3-(3-methoxybenzyl)-5-methyleneoxazolidin-2-one:** ^{1}H NMR (400 MHz, $CDCl_3$), δ (ppm): 7.28-7.25 (m, 1H), 6.85-6.78 (m, 3H), 4.72-4.71 (q, 1H), 4.41 (s, 2H), 4.22-4.21 (q, 1H), 4.01 (t, 2H), 3.78 (s, 3H), ^{13}C NMR (100 MHz, $CDCl_3$), δ (ppm): 159.98, 155.59, 148.85, 136.41, 129.96, 120.30, 113.61, 113.57, 86.76, 55.23, 47.73, 47.17.

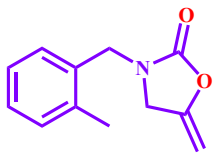	**3-(2-methylbenzyl)-5-methyleneoxazolidin-2-one:** ^{1}H NMR (400 MHz, $CDCl_3$), δ (ppm): 7.21 (d, 1H), 7.15 (d, 1H), 7.09-7.01 (m, 2H), 4.72-4.71 (q, 1H), 4.39 (s, 2H), 4.22-4.21 (q, 1H), 3.91 (t, 2H), 2.31 (s, 3H), ^{13}C NMR (100 MHz, $CDCl_3$), δ (ppm): 155.55, 148.91, 144.95, 129.96, 129.55, 128.11, 124.91, 86.56, 47.83, 46.93, 21.17.
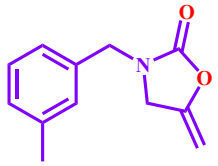	**3-(3-methylbenzyl)-5-methyleneoxazolidin-2-one:** ^{1}H NMR (400 MHz, $CDCl_3$), δ (ppm): 7.25-7.15 (m, 4H), 4.72-4.71 (q, 1H), 4.49 (s, 2H), 4.22-4.21 (q, 1H), 3.95 (t, 2H), 2.31 (s, 3H), ^{13}C NMR (100 MHz, $CDCl_3$), δ (ppm): 155.18, 149.92, 136.75, 132.51, 130.96, 128.92, 128.35, 126.11, 86.96, 47.13, 45.93, 18.97.
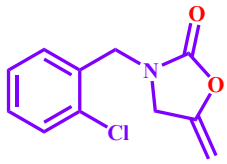	**3-(2-chlorobenzyl)-5-methyleneoxazolidin-2-one:** ^{1}H NMR (400 MHz, $CDCl_3$), δ (ppm): 7.45-7.35 (m, 2H), 7.33-7.25 (m, 3H), 4.72-4.71 (q, 1H), 4.61 (s, 2H), 4.28-4.27 (q, 1H), 4.11 (t, 2H). ^{13}C NMR (100 MHz, $CDCl_3$), δ (ppm): 155.81, 148.95, 133.95, 132.51, 130.16, 129.91, 129.51, 127.57, 86.96, 47.53, 44.97.

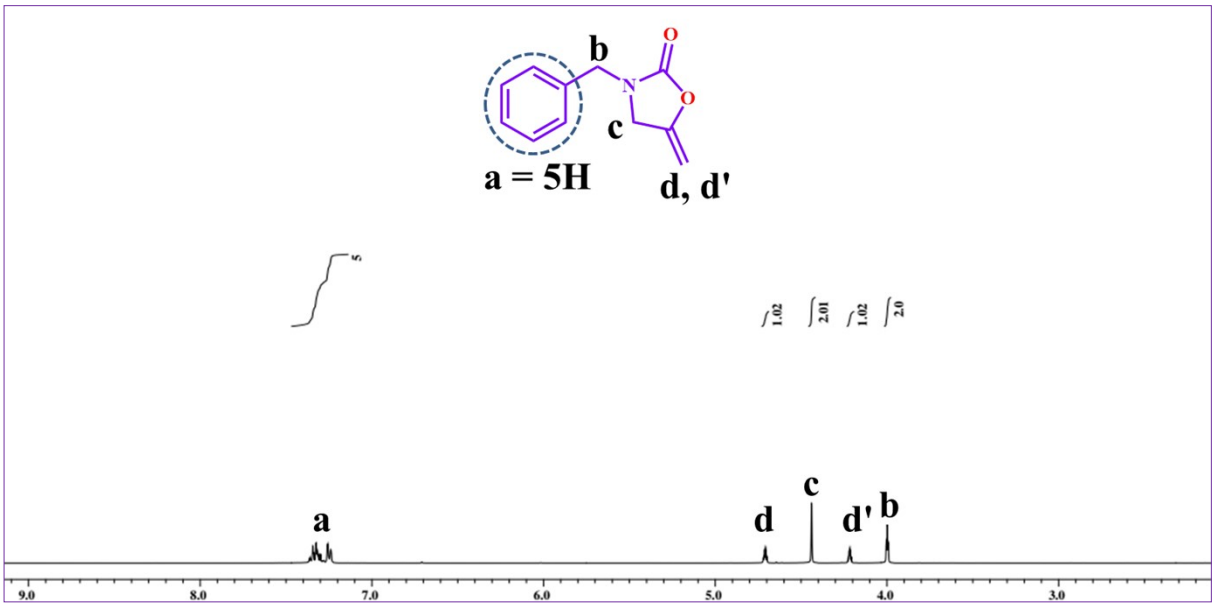

Figure S46. ^{1}H NMR ($CDCl_3$, 400 MHz) spectra of 3-Benzyl-5-methyleneoxazolidin-2-one catalyzed by Co-COF under the optimized conditions.

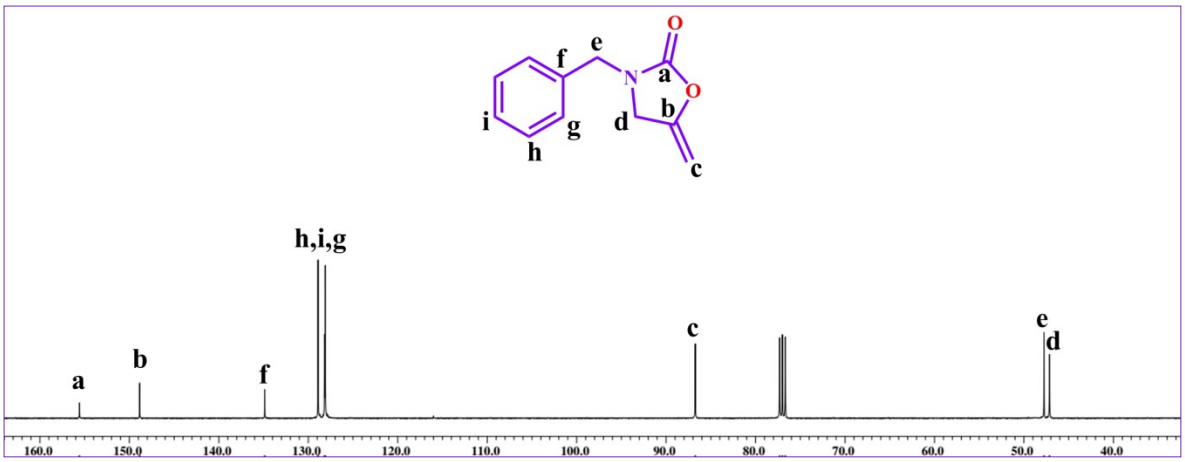

Figure S47. ^{13}C NMR ($CDCl_3$, 100 MHz) spectra of 3-Benzyl-5-methyleneoxazolidin-2-one catalyzed by Co-COF under the optimized conditions.

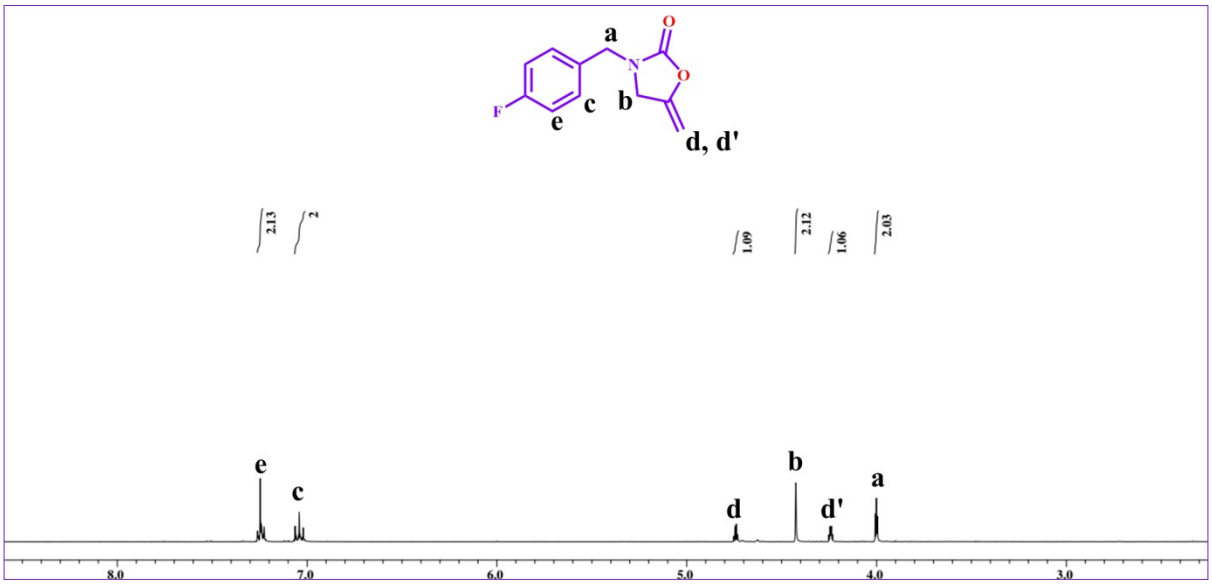

Figure S48. ^{1}H NMR ($CDCl_3$, 400 MHz) spectra of 3-(4-Fluorophenyl)-5-methyleneoxazolidin-2-one catalyzed by Co-COF under the optimized conditions.

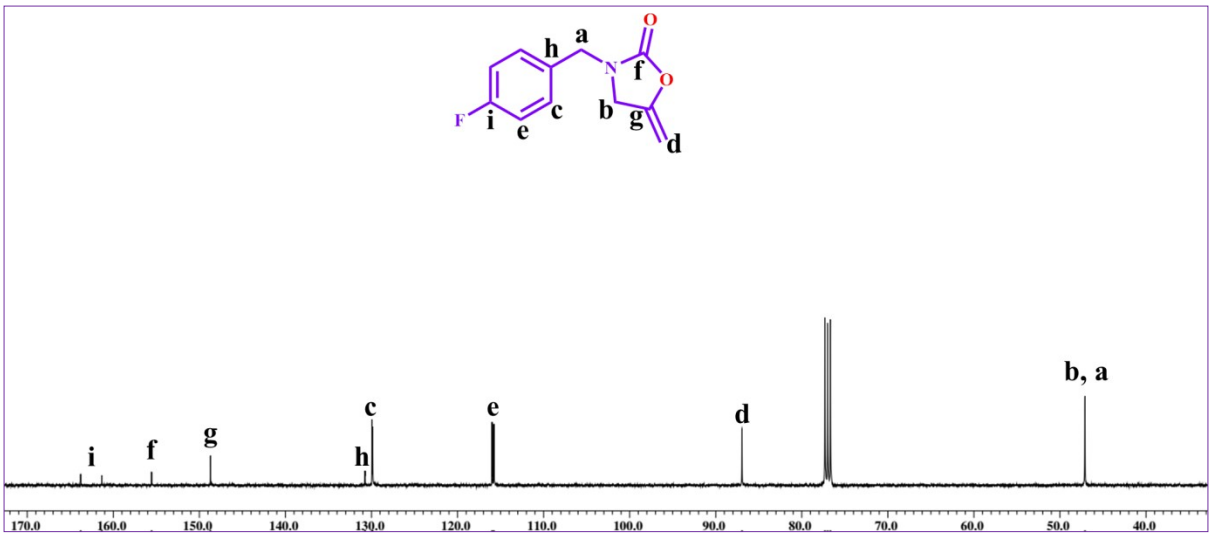

Figure S49. ^{13}C NMR ($CDCl_3$, 100 MHz) spectra of 3-(4-Fluorophenyl)-5-methyleneoxazolidin-2-one catalyzed by Co-COF under the optimized conditions.

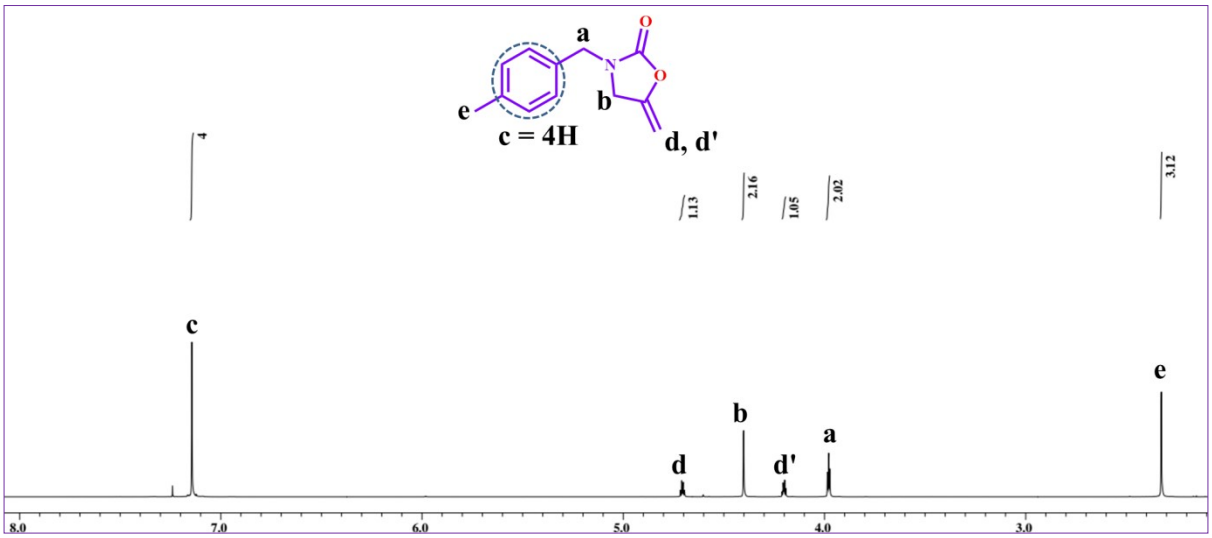

Figure S50. ^{1}H NMR ($CDCl_3$, 400 MHz) spectra of 3-(4-Methylphenyl)-5-methyleneoxazolidin-2-one catalyzed by Co-COF under the optimized conditions.

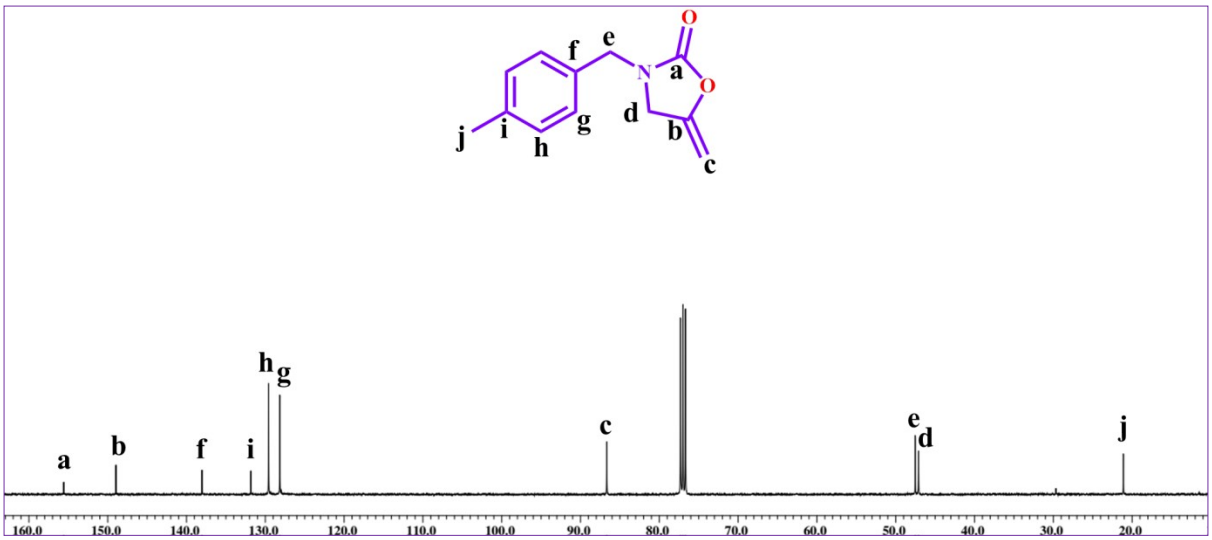

Figure S51. ^{13}C NMR ($CDCl_3$, 100 MHz) spectra of 3-(4-Methylphenyl)-5-methyleneoxazolidin-2-one catalyzed by Co-COF under the optimized conditions.

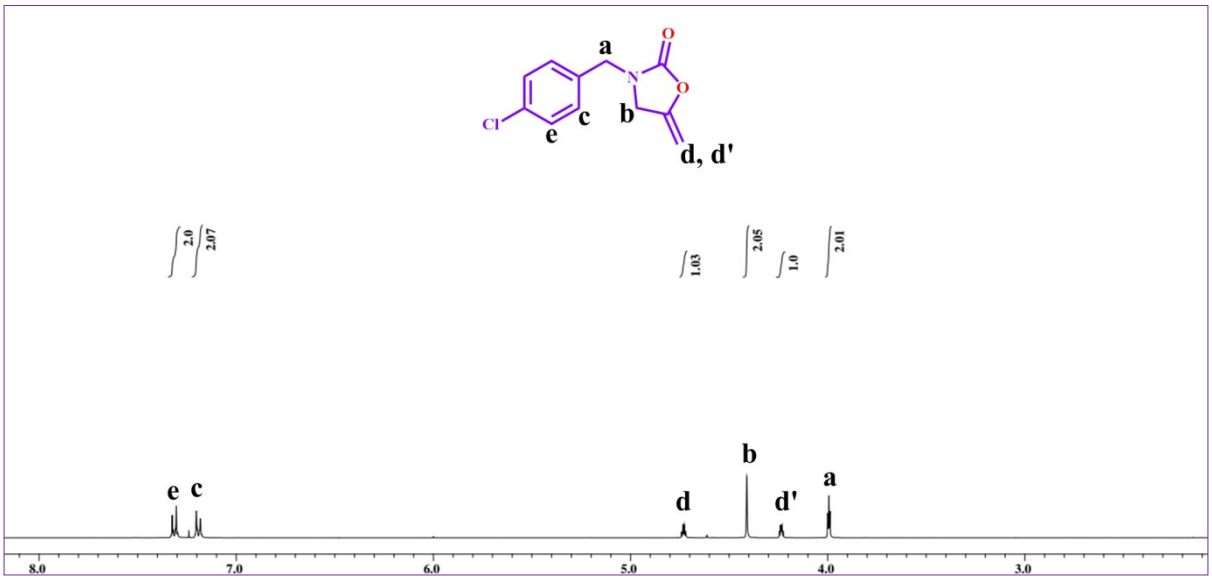

Figure S52. ^{1}H NMR ($CDCl_3$, 400 MHz) spectra of 3-(4-Chlorophenyl)-5-methyleneoxazolidin-2-one catalyzed by Co-COF under the optimized conditions.

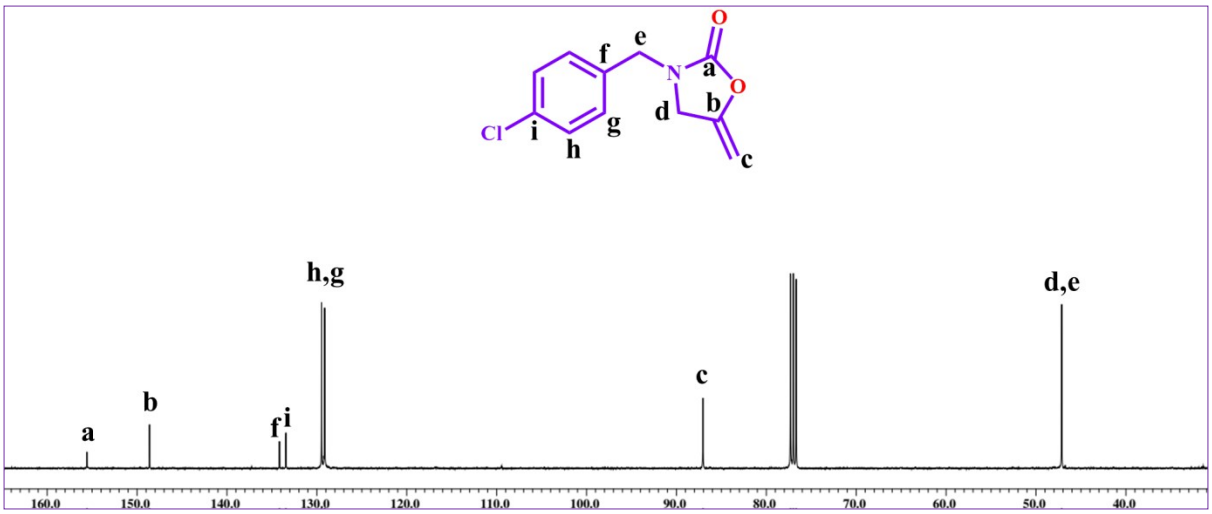

Figure S53. ^{13}C NMR ($CDCl_3$, 100 MHz) spectra of 3-(4-Chlorophenyl)-5-methyleneoxazolidin-2-one catalyzed by Co-COF under the optimized conditions.

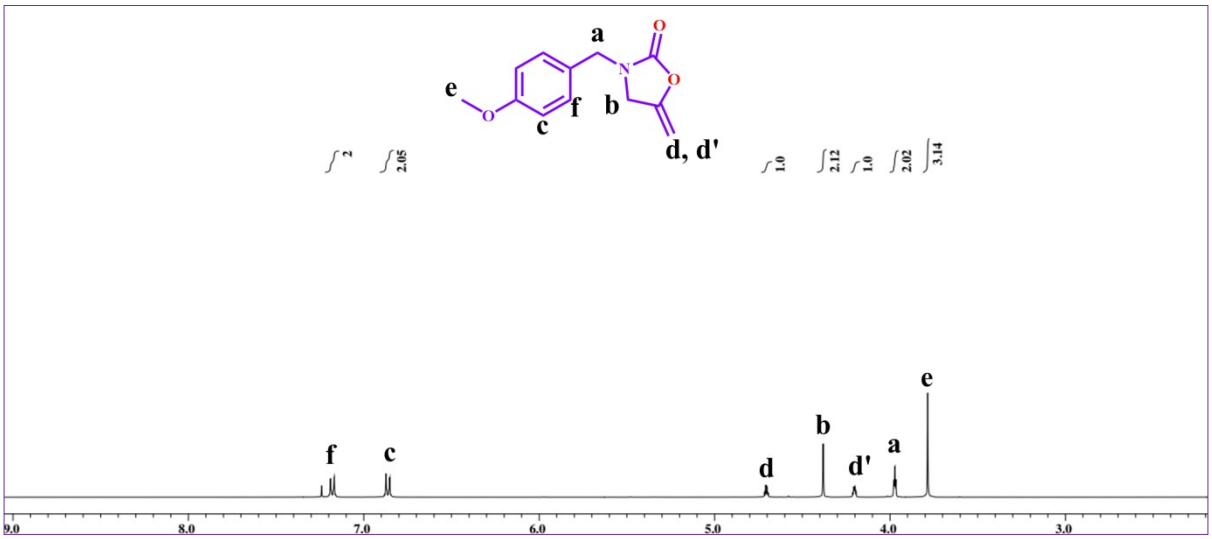

Figure S54. ^{1}H NMR ($CDCl_3$, 400 MHz) spectra of 3-(4-Methoxyphenyl)-5-methyleneoxazolidin-2-one catalyzed by Co-COF under the optimized conditions.

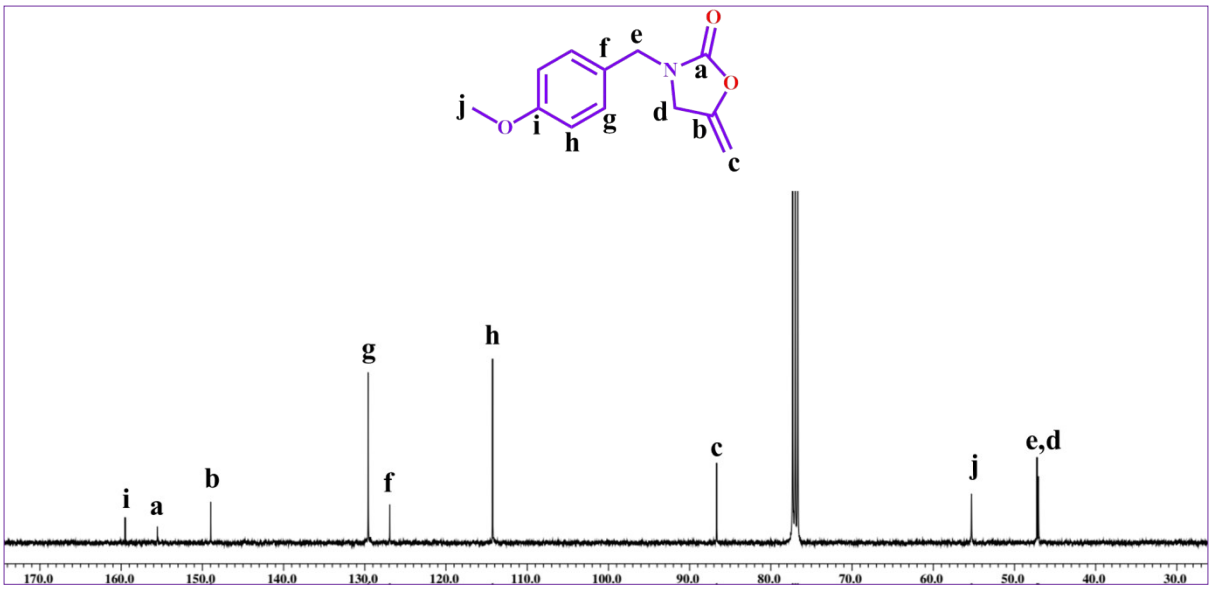

Figure S55. ^{1}H NMR ($CDCl_3$, 400 MHz) spectra of 3-(4-Methoxyphenyl)-5-methyleneoxazolidin-2-one catalyzed by Co-COF under the optimized conditions.

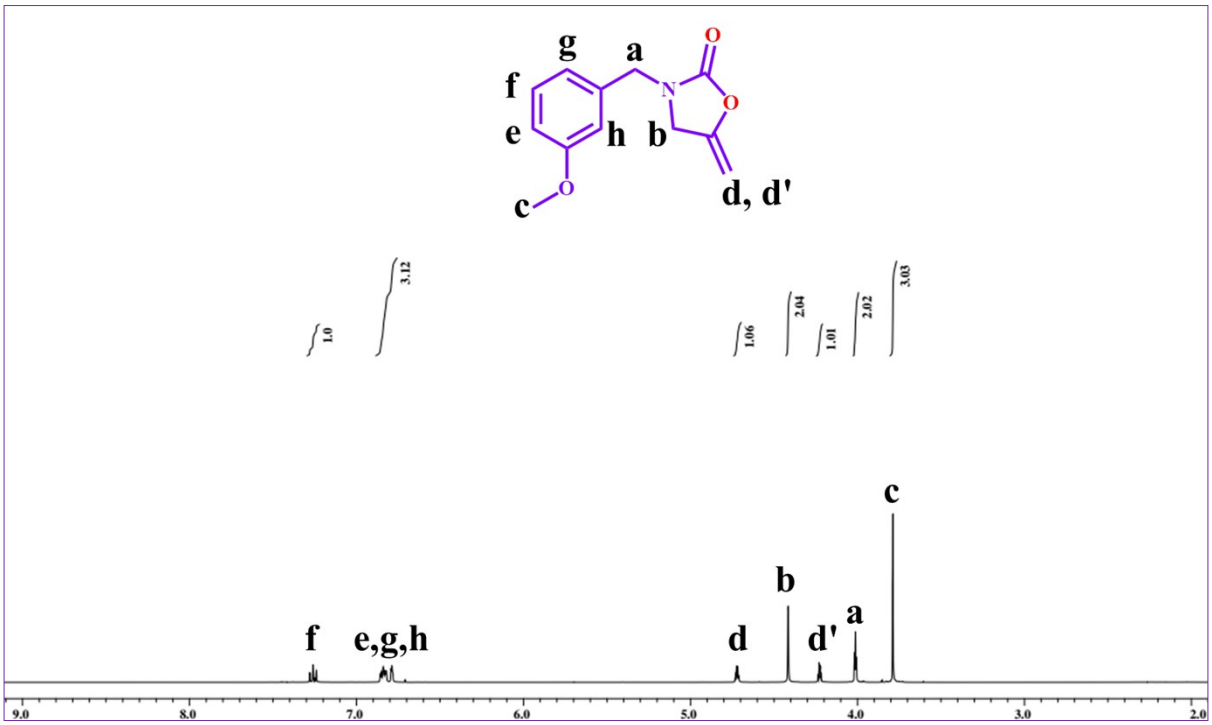

Figure S56. ^{1}H NMR ($CDCl_3$, 400 MHz) spectra of 3-(3-methoxybenzyl)-5-methyleneoxazolidin-2-one catalyzed by Co-COF under the optimized conditions.

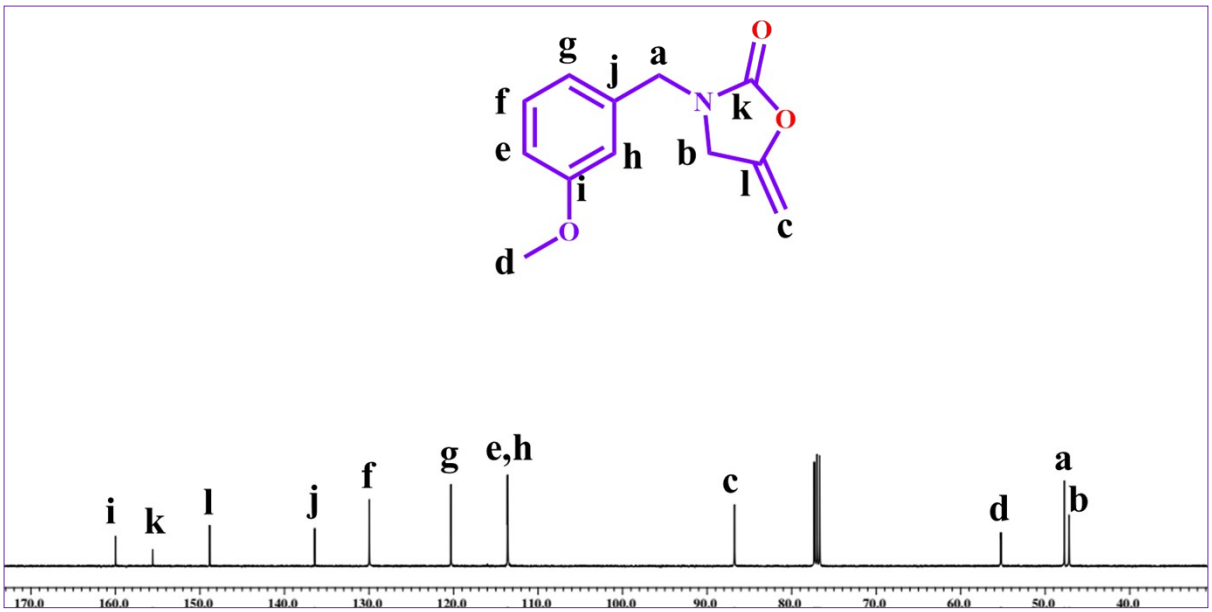

Figure S57. ^{1}H NMR ($CDCl_3$, 400 MHz) spectra of 3-(3-methoxybenzyl)-5-methyleneoxazolidin-2-one catalyzed by Co-COF under the optimized conditions.

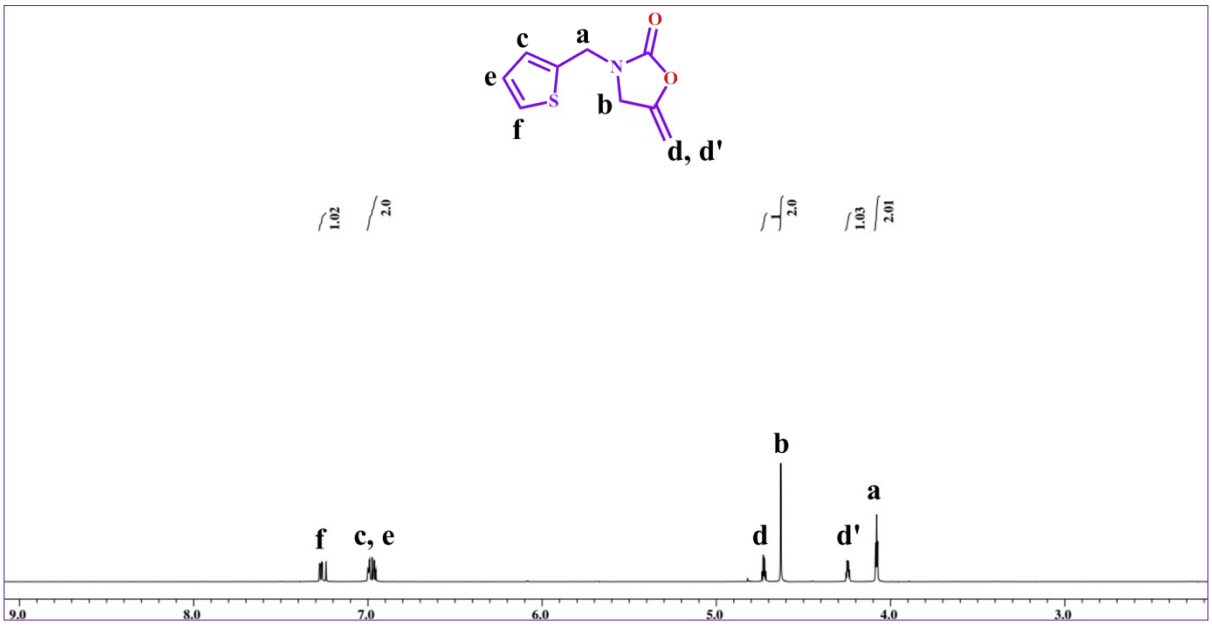

Figure S58. ^{1}H NMR ($CDCl_3$, 400 MHz) spectra of 5-methylene-3-(thiophen-2-ylmethyl)oxazolidin-2-one catalyzed by Co-COF under the optimized conditions.

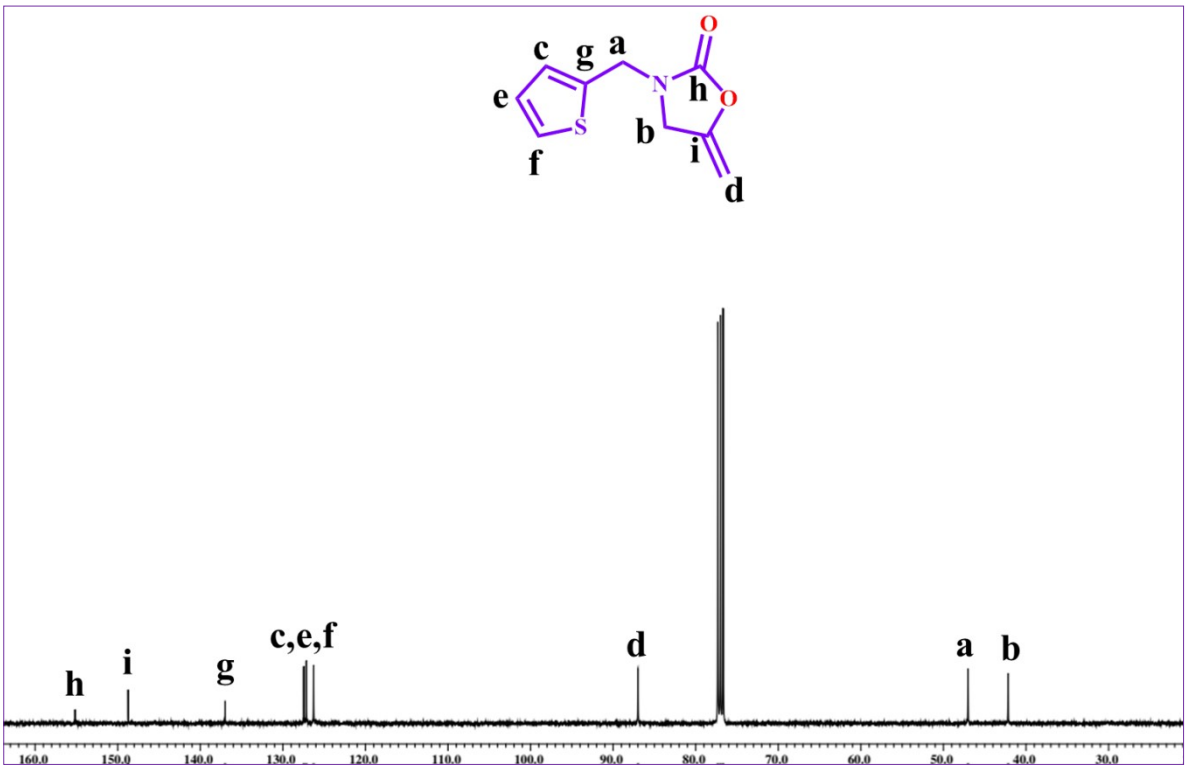

Figure S59. ^{13}C NMR ($CDCl_3$, 100 MHz) spectra of 5-methylene-3-(thiophen-2-ylmethyl)oxazolidin-2-one catalyzed by Co-COF under the optimized conditions.

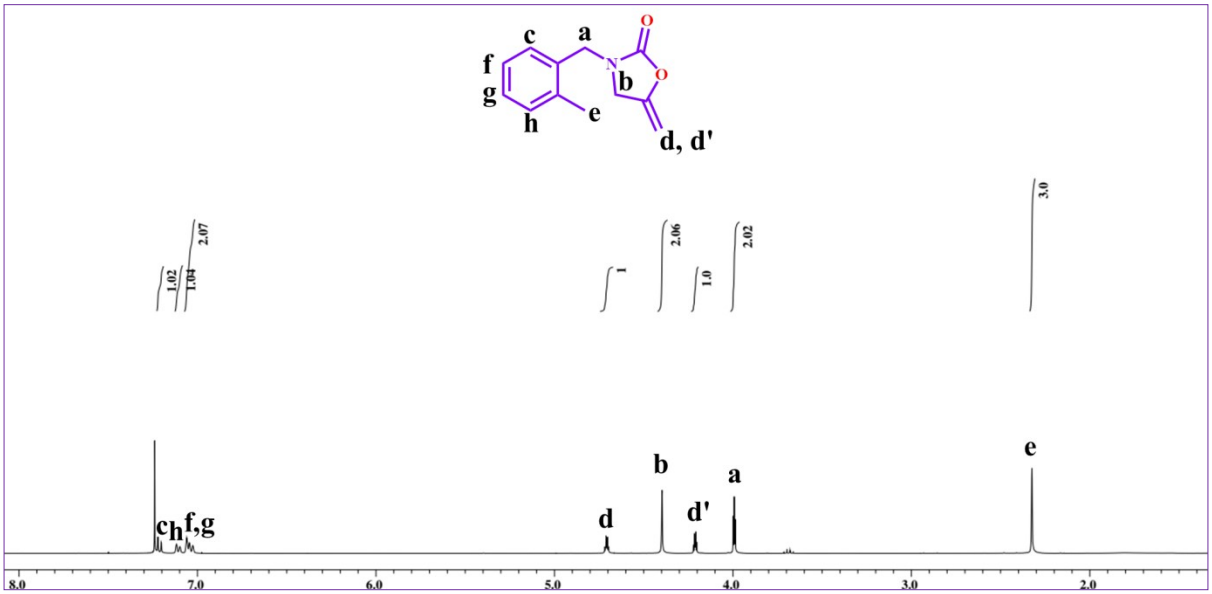

Figure S60. ^{1}H NMR ($CDCl_3$, 400 MHz) spectra of 3-(2-methylbenzyl)-5-methyleneoxazolidin-2-one catalyzed by Co-COF under the optimized conditions.

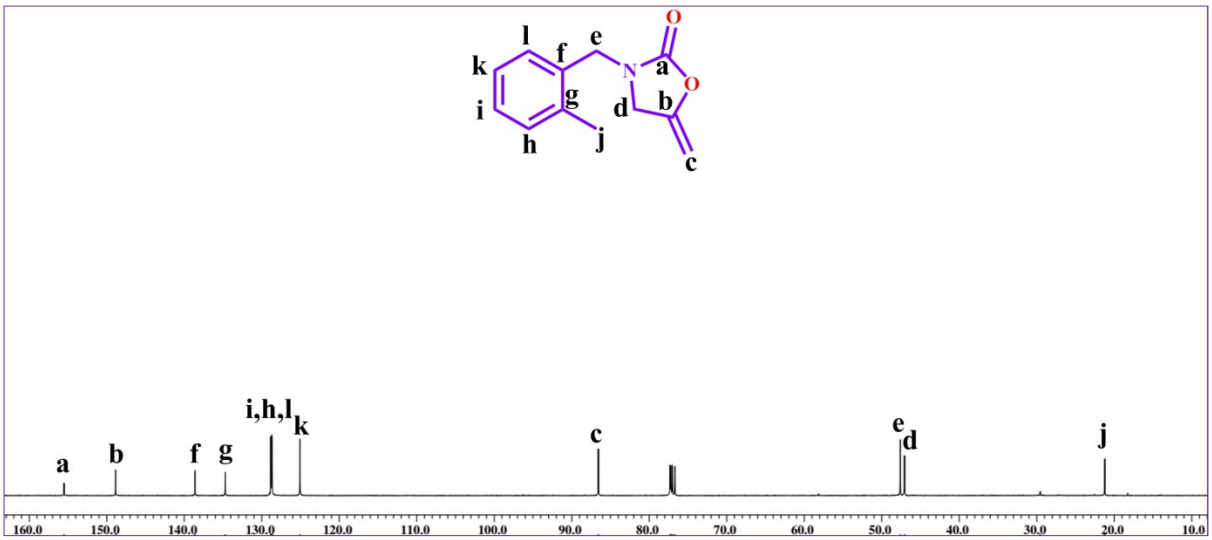

Figure S61. ^{13}C NMR ($CDCl_3$, 100 MHz) spectra of 3-(2-methylbenzyl)-5-methyleneoxazolidin-2-one catalyzed by Co-COF under the optimized conditions.

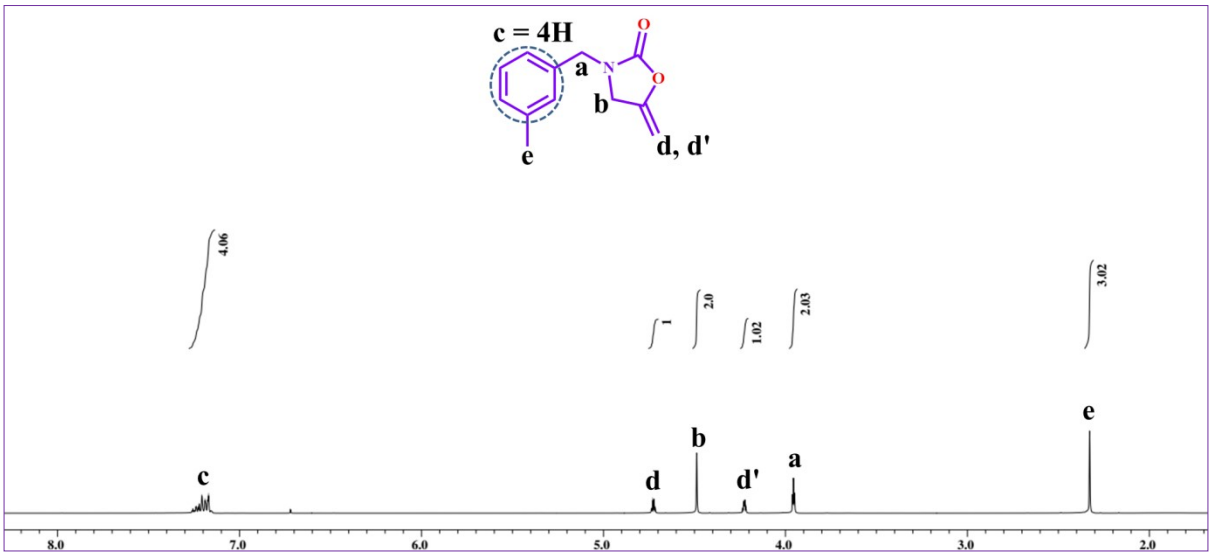

Figure S62. ^{1}H NMR ($CDCl_3$, 400 MHz) spectra of 3-(3-methylbenzyl)-5-methyleneoxazolidin-2-one catalyzed by Co-COF under the optimized conditions.

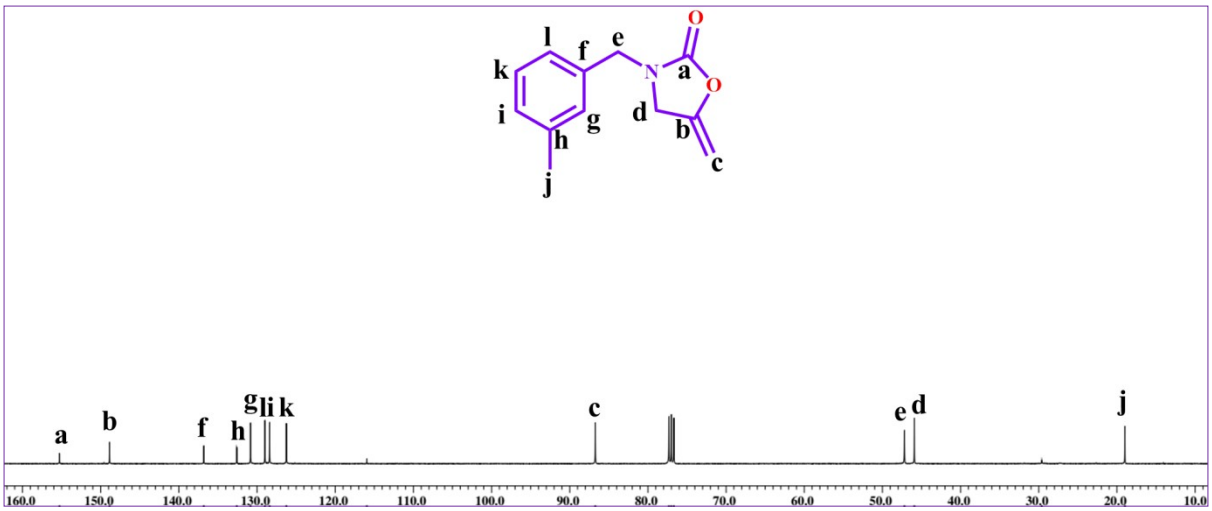

Figure S63. ^{13}C NMR ($CDCl_3$, 100 MHz) spectra of 3-(3-methylbenzyl)-5-methyleneoxazolidin-2-one catalyzed by Co-COF under the optimized conditions.

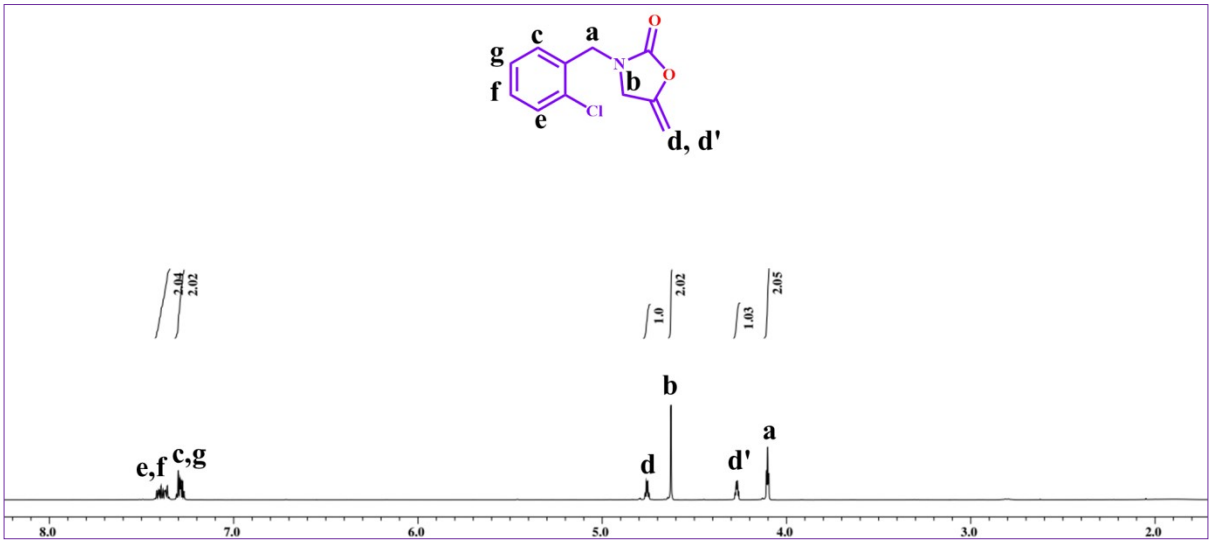

Figure S64. ^{1}H NMR ($CDCl_3$, 400 MHz) spectra of 3-(2-chlorobenzyl)-5-methyleneoxazolidin-2-one catalyzed by Co-COF under the optimized conditions.

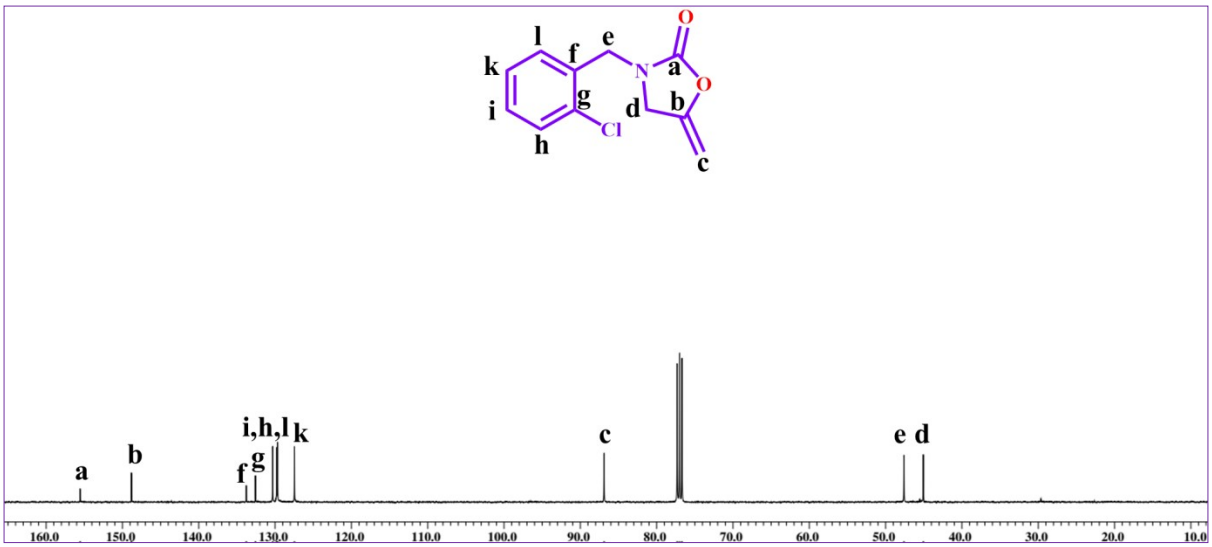

Figure S65. ^{13}C NMR ($CDCl_3$, 100 MHz) spectra of 3-(2-chlorobenzyl)-5-methyleneoxazolidin-2-one catalyzed by Co-COF under the optimized conditions.

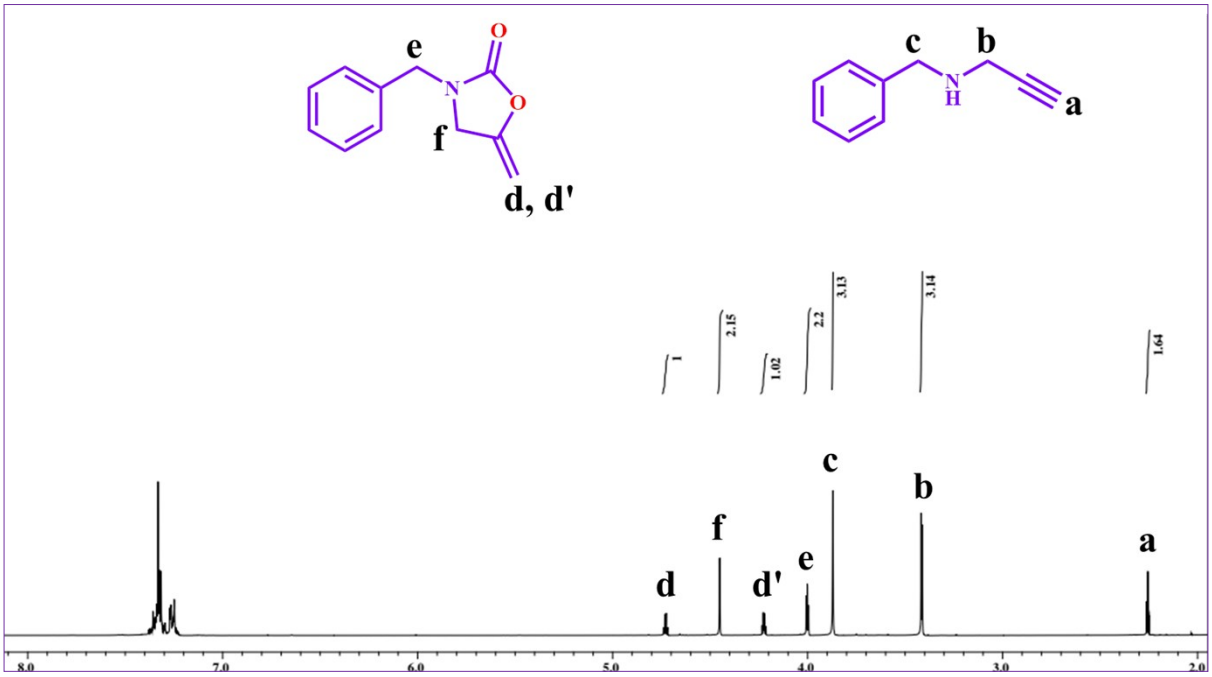

Figure S66. ^{1}H NMR ($CDCl_3$, 400 MHz) spectra for the cyclic carboxylation of N-benzylprop-2-yn-1-amine catalyzed by Co-COF using simulated flue gas (13:87 % = CO_2:N_2) under the optimized conditions.

Table S8. Comparison of the catalytic activity of Co-COF with the reported catalysts for the carboxylative cyclization of propargylic amines with CO_2 to form 2-oxazolidinones.

Sl. No.	Catalyst	Active Sites	Temp. (°C)	Yield (%)	Ref.
1.	Cd-BPy-COF	Cd	60	99	10
2.	AgN@COF	Ag(0)	55	94	11
3.	Cu-NPs@COF	Cu(0)	50	95	12
4.	Ag@NPOP-1	Ag(0)	50	97	13
5.	Ag@NPOP-2	Ag(0)	50	93	13
6.	Ag@2,6-FPP-TAPT	Ag(0)	50	99	14
7.	Ag@2,6-FPP-TAPT	Ag(0)	50	91	14
8.	Ag@Pybpy-COF	Ag(0)	50	99	15
9.	CuTp-BD-COF	Cu(I)	80	99	16
10.	**Co-COF**	**Co(II)**	**40**	**99**	**This work**

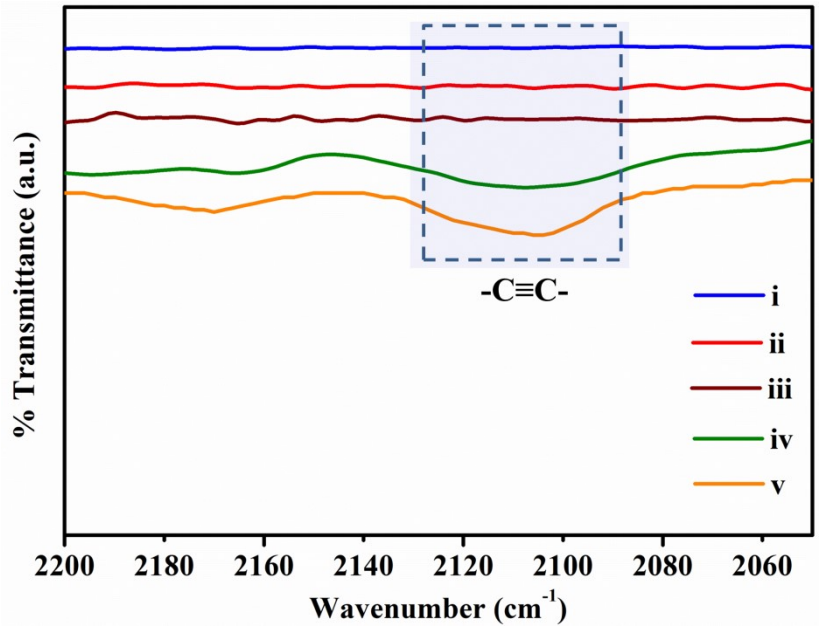

Figure S67. FT-IR spectra of (i) EtDh-COF, (ii) EtDh-COF treated with N-benzylprop-2-yn-1-amine, (iii) Co-COF, (iv) Co-COF treated with N-benzylprop-2-yn-1-amine, and (v) N-benzylprop-2-yn-1-amine.

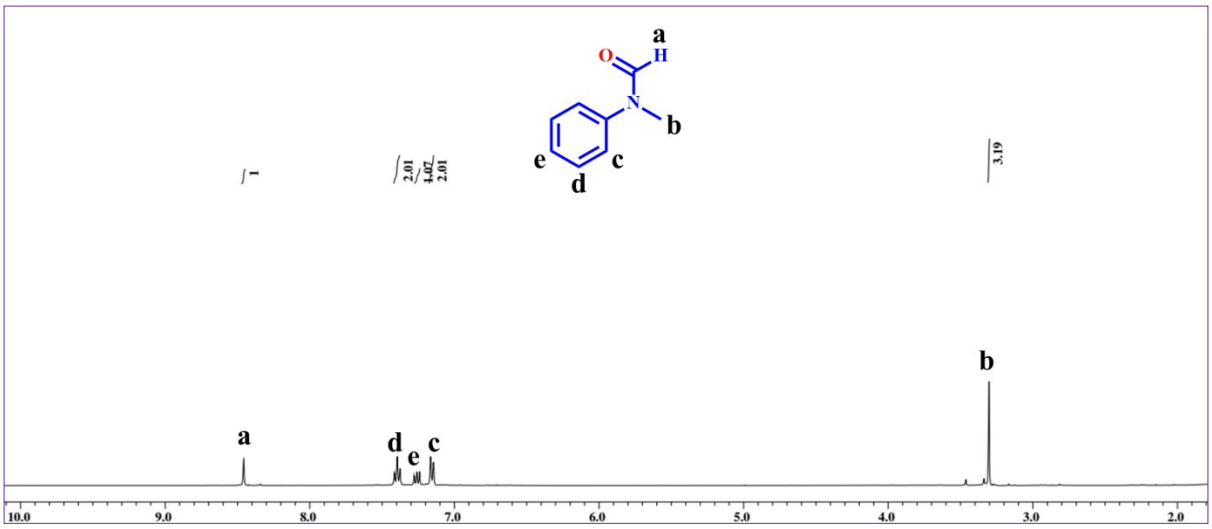

Figure S68. ^{1}H NMR ($CDCl_3$, 400 MHz) spectra of N-methylformanilide catalyzed by Co-COF recycled after four cycles under the optimized conditions.

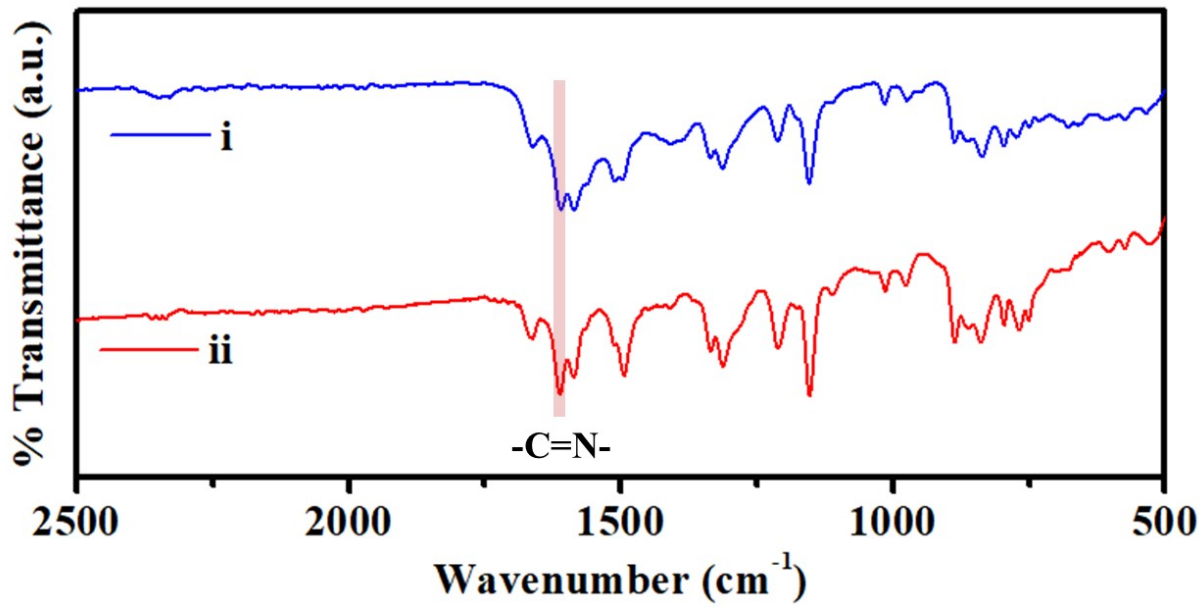

Figure S69. FT-IR spectra of (i) Co-COF and (ii) recovered after five cycles of catalysis.

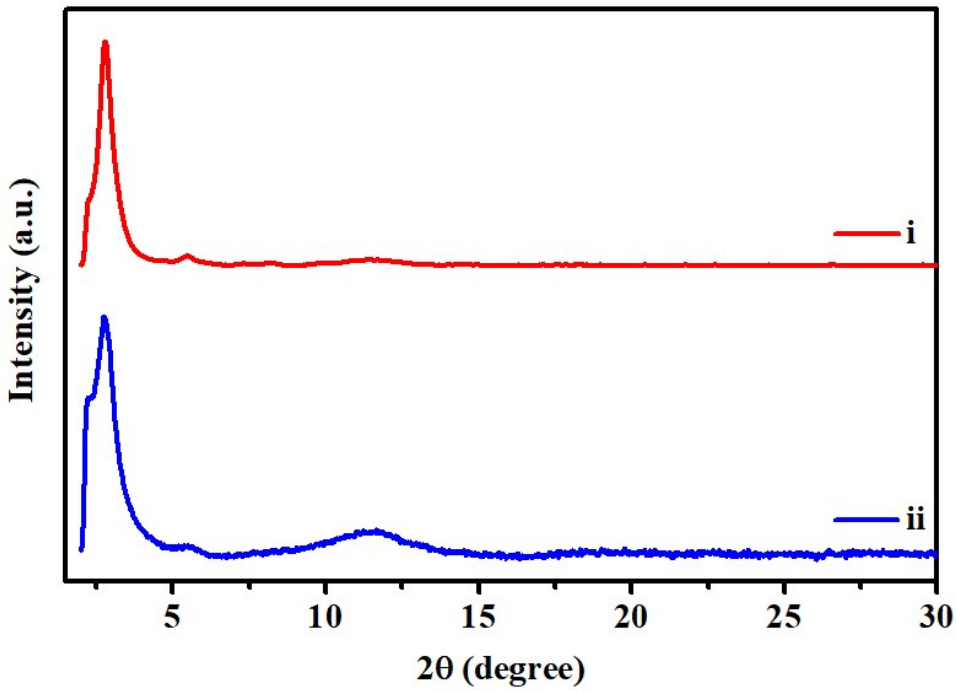

Figure S70. Powder XRD plots of (i) Co-COF, and (ii) recovered after five cycles of catalysis.

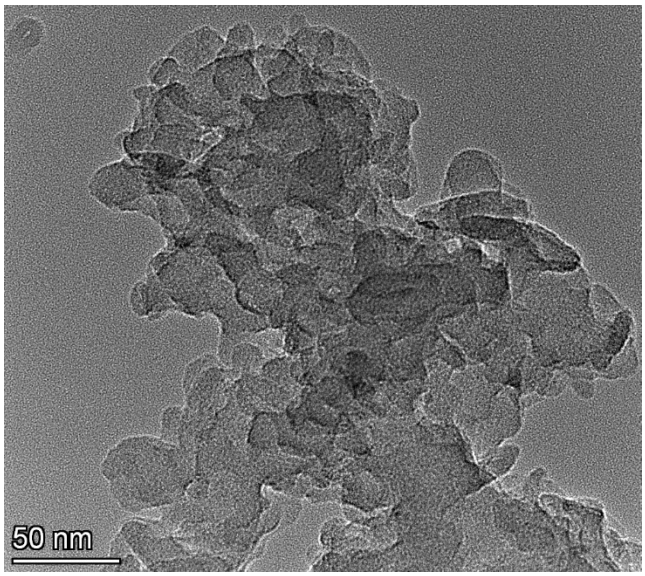

Figure S71. HR-TEM image of recycled Co-COF.

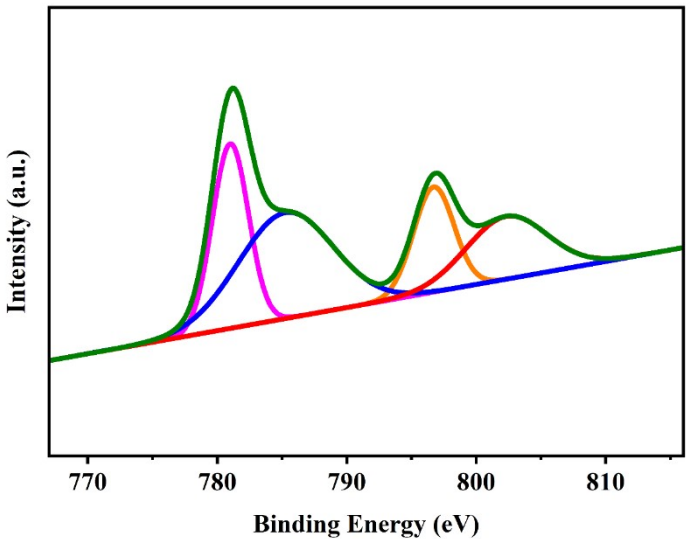

Figure S72. XPS plot of recycled Co-COF

References

1. Z. -F. Pang, T. -Y. Zhou, R. -R. Liang, Q. -Y. Qi and X. Zhao, Regulating the topology of 2D covalent organic frameworks by the rational introduction of substituents, *Chem. Sci.*, 2017, **8**, 3866-3870.

2. H. Pan, J. A. Ritter and P. B. Balbuena, Examination of the Approximations Used in Determining the Isosteric Heat of Adsorption from the Clausius-Clapeyron Equation, *Langmuir*, 1998, **14**, 6323-6327.

3. R. T. Yang, Gas Separation by Adsorption Processes, Butterworth, Boston, 1997.

4. Z. Zhou, X. Liu, J. -G. Ma and P. Cheng, MOF-Incorporated Binuclear N-Heterocyclic Carbene-Cobalt Catalyst for Efficient Conversion of CO_2 to Formamides, *ChemSusChem*, 2022, **15**, e202201386.

5. J. W. Liu, Y. Z. Fan, K. Zhang, L. Zhang and C. Y. Su, Engineering Porphyrin Metal-Organic Framework Composites as Multifunctional Platforms for CO_2 Adsorption and Activation, *J. Am. Chem. Soc*., 2020, **142**, 14548-14556.

6. B. Dong, L. Wang, S. Zhao, R. Ge, X. Song, Y. Wang and Y. Gao, Immobilization of ionic liquids to covalent organic frameworks for catalyzing the formylation of amines with CO_2 and phenylsilane, *Chem. Commun.*, 2016, **52**, 7082-7085.

7. X. Kang, Z. Wang, X. Shi, X. Jiang, Z. Liu and B. Zhao, Effective Reduction of CO_2 with Aromatic Amines into N-Formamides Triggered by Noble-Free Metal-Organic Framework Catalysts Under Mild Conditions, *Small*, 2024, **20**, 2311511.

8. Q. Cao, L. -L. Zhang, C. Zhou, J. -H. He, A. Marcomini and J. -M. Lu, Covalent Organic Framework-supported Zn single atom catalyst for highly efficient N-formylation of amines with CO_2 under mild conditions, *Appl. Catal. B: Environ.*, 2021, **294**, 120238.

9. Z. -Q. Wang, C. –H. Deng, X. Liu and W. –M. Wang, Highly efficient conversion of CO_2

into N-formamides catalyzed by a noble-metal-free aluminum-based MOF under mild conditions, *Dalton Trans.*, 2023, **52**, 11163-11167.

10. Y. Zhang, H. Li, X. He, A. Wang, G. Bai and X. Lan, Covalent organic frameworks embedding single cadmium sites for efficient carboxylative cyclization of CO_2 with propargylic amines, *Green Chem.*, 2023, **25**, 5557-5565.

11. S. S. Islam, S. Biswas, R. Molla, N. Yasmin and S. K Islam, Green Synthesized AgNPs Embedded in COF: An Efficient Catalyst for the Synthesis of 2-Oxazolidinones and α-Alkylidene Cyclic Carbonates via CO_2 Fixation, *ChemNanoMat*, 2020, **6**, 1386.

12. R. Khatun, S. Biswas, I. H. Biswas, S. Riyajuddin, N. Haque, K. Ghosh and S. M. Islam, Cu-NPs@COF: A potential heterogeneous catalyst for CO_2 fixation to produce 2-oxazolidinones as well as benzimidazoles under moderate reaction conditions, *J. CO_2 Util.*, 2020, **40**, 101180.

13. J. Wu, S. Ma, J. Cui, Z. Yang and J. Zhang, Nitrogen-Rich Porous Organic Polymers with Supported Ag Nanoparticles for Efficient CO_2 Conversion, *Nanomater*ials, 2022, **12**, 3088.

14. Y. Zhang, X. Lan, F. Yan, X. He, J. Wang, L. Ricardez-Sandoval, L. Chen and G. Bai, Controllable encapsulation of silver nanoparticles by porous pyridine-based covalent organic frameworks for efficient CO_2 conversion using propargylic amines, *Green Chem.*, 2022, **24**, 930-940.

15. G. Singh, N. Duhan, T. J. D. Kumar and C. M. Nagaraja, Pyrene-Based Nanoporous Covalent Organic Framework for Carboxylation of C-H Bonds with CO_2 and Value-Added 2-Oxazolidinones Synthesis under Ambient Conditions, *ACS Appl. Mater. Interfaces*, 2024, **16**, 5857-5868.

16. J. Qiu, X. Qi, K. Zhu, Y. Zhao, H. Wang, Z. Li, H. Wang, Y. Zhaoa and J. Wang, Cu^{I}-anchored porous covalent organic frameworks for highly efficient conversion of propargylic

amines with CO_2 from flue gas, *Green Chem.*, 2024, **26**, 6172-6179.